RSC Advances

ROYAL SOCIETY OF CHEMISTRY

www.rsc.org/advances

Journal Name

ARTICLE

Recent advances in hybrid periodic mesostructured organosilica materials: opportunities from fundamental to biomedical applications

Received 00th January 20xx,
Accepted 00th January 20xx

DOI: 10.1039/x0xx00000x

www.rsc.org/

Mohammad A. Wahab* and Jorge N. Beltramini

Surfactant-mediated periodic mesoporous organosilicas (PMOs) with different organic and inorganic functions in the framework structure have been discovered in 1999, whereas the silica inorganic function gives a strong mechanical stability to the framework structure and the organic functionality creates more structural flexibility. As a result, their use is optimal for larger number of applications including catalysis, microelectronics, chromatographic supports, selective adsorbents, sensors, protein folding, biomedical and light-harvesting devices. These new materials showed also superior stability when compared to pure mesoporous silica (PMS) framework structures. Based on the recent discoveries, since 2012, this review mostly provides a comprehensive overview of their multidisciplinary options for various applications.

1. Introduction

Mesoporous materials synthesized *via* self-assembly technique are widely used in advanced applications such as: optoelectronics, light harvesting, biomedical, sensors, catalysts, environmental, and nanobiotechnology.[1-24] Their use depends on the pore size and shape and on the presence of functional groups in their final mesoporous framework.[5-22] In 1992, the discovery of pure mesoporous silica structures (known as MCM41, where MCM stands Mobil Composition of Matter) *via* the surfactant-mediated self-assembly synthesis of surfactant micelles and tetraethyl orthosilicate (TEOS) has expanded the applications of microporous molecular sieves beyond the 1-2 nm restrictions.[1] At the same time, by changing the surfactant concentration and synthesis temperatures a new kind of ordered mesoporous silica materials including MCM48 (cubic pore) and MCM50 (lamellar/layered) were also reported.[1] The removal of the surfactant micelles by calcination or solvent extraction leaves behind well-ordered porous mesostructured silica (PMS) structures with pores diameters ranging from 2 to 5 nm and specific surface areas of about 900-1000 m^2/g. In 1998, silica based SBA15 and associated similar kind of structures with different wall thicknesses were also reported.[16,11-24] Efforts were also made to overcome the neutral nature of inorganic mesoporous silica framework by functionalization with various functional groups to expand their applications in different research areas.[1-34] Another important limitation that concerns with the hydro-thermal stability of PMS structures is when they are present a in water/aqueous medium. For example, if MCM41/MCM48 samples are exposed to boiling water for 12 h then they will completely loss their framework structure due to the hydrolysis of the silicate walls (Si-O-Si). Hence, these mesoporous silica structural limitations made necessary the design and development of new alternative materials that can overcome the aforementioned drawbacks.[1-5,15-30] In this context, hybrid PMOs prepared by self-assembling organic and inorganic units (Fig. 1) in a single material framework can easily overcome the limitation problems found on PMS materials.[5,15-23,40-84] Significantly, the presence of inorganic Si function in the framework structure

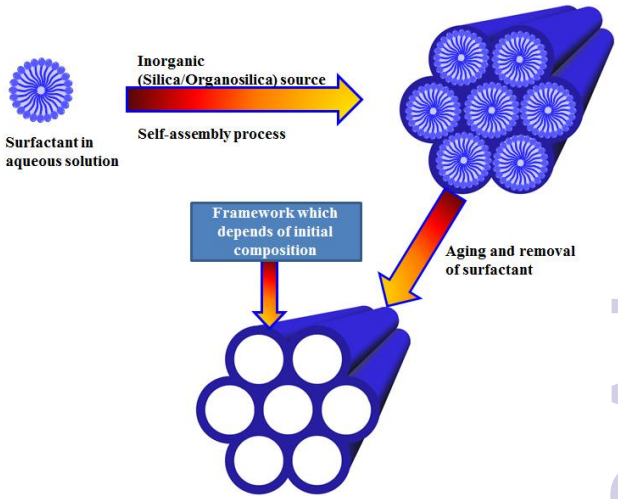

Fig. 1. General self-assembly method for preparing PMOs. Framework composition of the final PMOs depends on the initial reactant components.

[a] Nanomaterials Centre, Australian Institute for Bioengineering and Nanotechnology, The University of Queensland, Brisbane, St Luica, Qld 4073, Australia. *E-mail: m.wahab@uq.edu.au /j.beltramini@uq.edu.au

† Footnotes relating to the title and/or authors should appear here. Electronic Supplementary Information (ESI) available: [details of any supplementary information available should be included here]. See DOI: 10.1039/x0xx00000x

usually builds a robust framework while organic functions make frameworks more flexible in a way so that PMOs can be possible tailored in a number of important applications.[20-105] For the comfort of the reader, a list of acronyms used in this review is outlined at the end of text.

2. Limitations of pure mesoporous silicas lead to discover PMOs

2.1 Functionalization of mesoporous silica framework

Two synthesis techniques were used that can explain the functionality of various PMOs. Firstly, co-condensation method (Fig. 2) which is associated with the co-assembling of TEOS with an organosiloxane of the type $RSi(OEt)_3$ (R stands for organic group and OEt stands for ethoxy group) in the presence of surfactant under acid or basic conditions, and, secondly post-grafting technique (Fig. 3) where the organic functional groups are usually incorporated onto the pore channel walls of mesoporous framework taking advantage of the reactivity of the surface silanol groups (Si-OH) present into the mesoporous structure.[15-18,20-26] As a result the organic groups became a part of the wall structure, providing functionality not only to its surface but to the entire mesoporous structure.[6-14,49-79] However, both methods suffer from inhomogeneous distribution of organic groups inside the pores that severely block the pore entrance due to the incompatibility of silica and organosilica structures. Most of the long chain containing trialkoxy-silsesquioxanes/silsesquioxanes cannot maintain a mesoporous structure after template removal and, being also unstable to the condensation conditions, undergo intramolecular cyclization or simple phase separation from template. When a higher amount of silsesquioxane materials is co-condensed with TEOS totally disordered/amorphous structures are obtained. As a result to control the efficient mesoporous functionalization and to avoid leaching out organic functional groups the amount of functional groups should be in the concentration range of 5-15 mol%.[3-5,17,18-32,24-37]

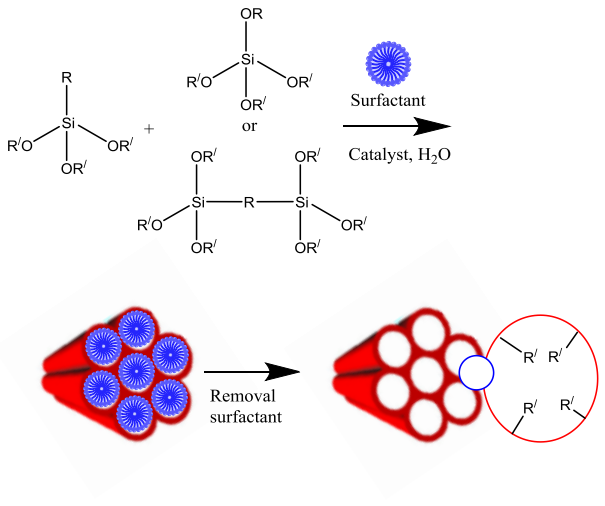

Fig. 2. Functionalization of mesoporous framework *via* direct co-condensation method under basic/acidic conditions. OR′ stands for ethoxy/methoxy groups.

2.2 Periodic Mesostructured Organosilicas (PMOs)

Due to the known limitations found on the mesoporous silica framework materials, three independent research groups (Inagaki, Stein and Ozin) in 1999 have reported for the first time the synthesis of PMO hybrids *via* surfactant-mediated self-assembly process under acid/basic conditions and using simple bridge organosilsesquioxane of the type $[(EtO)_3Si–R–Si(OEt)_3]$ as sole precursor as shown in Fig. 1.[40-52] As can be seen from Fig. 1, the PMOs could be synthesized using bridged silsesquioxanes groups such as $[(EtO)_3Si–R–Si(OEt)_3]$ as sole precursor, in which R is a functional group with a rigid structure such as ethane/benzene/biphenyl. R in $[(EtO)_3Si–R–Si(OEt)_3]$ groups should be rigid enough to undergo the surfactant self-assembly process. Afterwards, removing surfactant leaves behind a stable PMO structure with a high surface area along with a composition of $[_{1.5}OSi–R–SiO_{1.5}]$ groups where R is a key organic functional group which creates the flexibility, rigidity, and functionality of the framework of PMOs.[20-26,39-94] It is found that the study of bridged polysilsesquioxanes (BP) precedes invention of PMOs with different organic functionalities in the final framework. Bridged polysilsesquioxanes could also be obtained in the form of porous xerogels and aerogels with high surface areas (1000-1500 m^2/g). Those BPs are highly porous, transparent, and light-weight, and are useful as a matrix for growing metal and semiconductor nanoclusters or for optical applications such as waveguides, lasers, and nonlinear optics.[6-

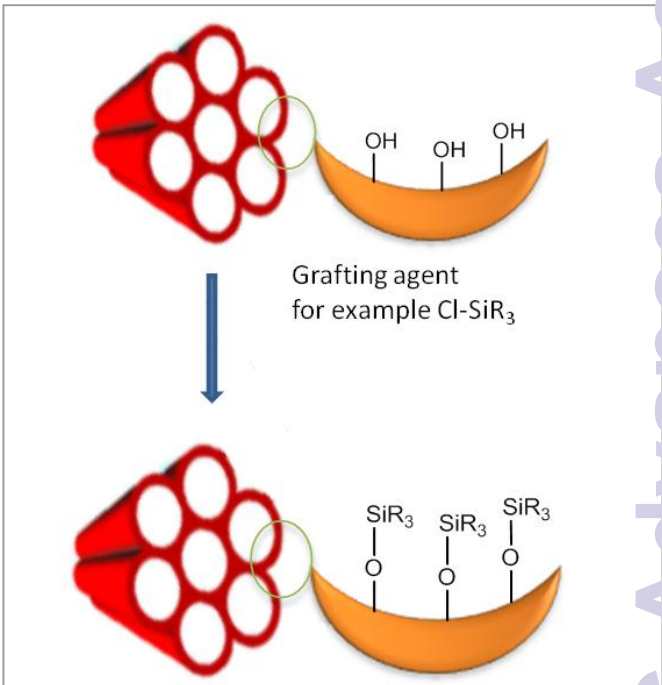

Fig. 3. Post-functionalization of mesoporous framework *via* post-grafting method.

[11,17-26] The important and key characteristic of a typical PMO synthesis is the use of a hydrolysable organosilane with a bridging organic group instead of a terminal one. The homogeneous distribution of organic and inorganic functions in the final framework of PMOs could easily be ensured whereas organic function is mainly responsible for creating unique advantages of PMOs.[6-11,17-26] The organic chemistry of pore walls of PMOs can easily facilitate the introduction of various organic functional groups into the pore channels and provides new opportunities for controlling the chemical, physical, optical, mechanical, surface, dielectric and overall properties of the PMOs. From the prospective point of PMOs, not only the mesoporosity of final PMO structure is what matters. Importantly, the chemical nature of the organic functions in the final PMO structures can also be tailored by the judicious choice of organic bridging groups for targeted applications. In addition, PMOs can reduce catalyst leaching and pore blockage whereas terminal group functionalized mesoporous structures are associated with inhomogeneous distribution of organic functions and leaching out cannot be ruled out during washing/solvent removing. However, as an example, a wide range of different PMOs functionalized with polysilylate molecular organosilica precursors with unique chemical, electrical, and optical properties have been synthesised.[20-26,44-104]

2.3 Chiral PMOs

Fig. 4 shows different types of chiral organosilane precursors that were used recently to prepare chiral PMOs with new chiral organosilane properties.[105-128] As previously reported, chiral organosilane functionalized PMOs showed circular dichroism (CD) or rotation of the polarization of linearly polarized light.[110,111] Crudden et al.[107] have shown that the synthesis of chiral PMOs based on axially chiral monomers modify the transmission of chirality in the solid state in which the π–π stacking interactions between aromatic systems in the solid state were prominent. A novel bistriethoxysilyl-binapthyl (BINAP) monomer was also co-condensed with a biphenylene-bridged organosilica in the presence of surfactant templates to prepare PMO functionalized with BINAP.[107] Complexion of ruthenium followed by asymmetric catalytic hydrogenation and asymmetric transfer hydrogenation were carried out to demonstrate that high levels of activity and selectivity can be achieved with the proposed chiral structure. In addition, it was found that the functional groups could also modify the morphologies and properties of the final product.[105-128]

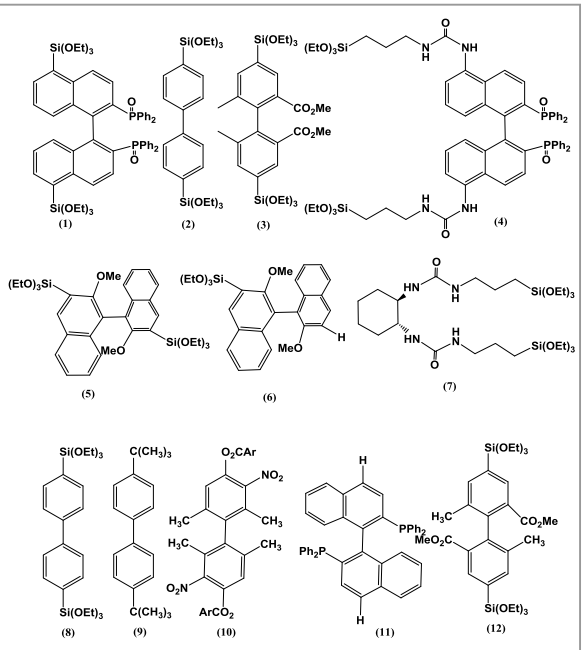

Fig. 4. Examples of chiral precursors have already been used for producing chiral PMOs, Reproduced from ref 105-107,124,129 with permission from ACS.

2.4 Morphology of PMO

Some applications depend on the shape and size of particles of PMOs for example, separation. Meanwhile, PMOs with various shapes including rods, fibres, spheres, gyroid, worm-like, and platelets have been also reported.[6-26,39-74] Selection of the synthesis parameters and post-treatment steps for PMOs enables to obtain the desired morphology and shape for a specific applications such as adsorbents, separation, catalysts and optical materials.[6-26,39-74] Hole-transport organosilica containing transparent PMO films *via* evaporation-induced self-assembly process have also been reported for optical and coating applications.[59]

3. Functional groups directed applications

It is important to note that the nature of organic groups present in mesoporous framework could easily change the functional properties and applications of the PMO structure.[6-26,39-84,129-170] PMOs with well-organized pore structures are very suitable for various applications such as heterogeneous catalysis, enzymatic catalysis, enzyme immobilization/adsorption and biomedical devices.[6-26,129-170] Meanwhile various studies have shown that the presence of textural properties (pore size and shape, functional groups, surface area and pore volume) in the PMOs are also very significant.[6-26] The following sections will focus on various applications/properties with respect to the functional inorganic/organic groups present in the PMOs framework reported since 2012. At the same time, sometimes other important examples will be invoked for the readers.

3.1 Heterogeneous catalysis

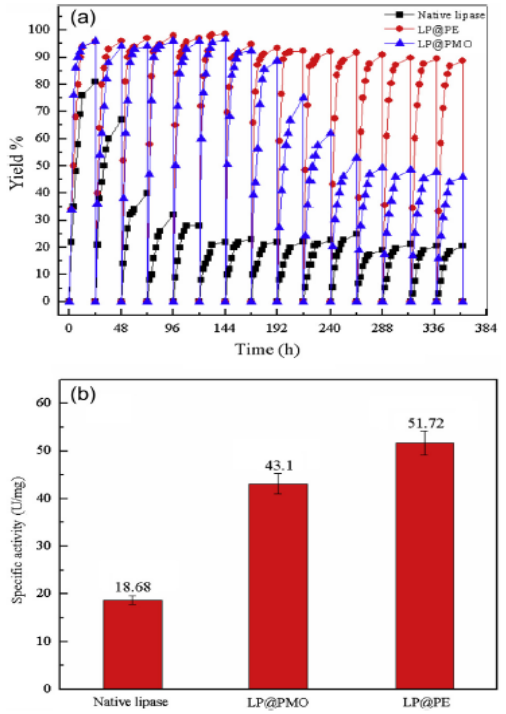

Fig. 5. The catalytic performance of LP@PE, LP@PMO and native lipase in esterification reactions (The reaction conditions: water fraction 0.65%, oleic acid 0.42 g, molar ratio of ethanol to oleic acid 2:1, LP@PMO 150 mg, phosphate buffer pH 7.0, 30 ^{O}C and 200 r/min). (b) The highest specific activity of LP@PE, LP@PMO and native lipase in esterification reactions, Reproduced from ref 130 with permission from Elsevier.

In a recent study, lipase-containing PMO particles were used to prepare Pickering emulsions.[130] Then the catalytic performance of LP@PE, LP@PMO and native lipase particles were tested for the catalytic esterification reaction of fatty acids into biodiesel using a water fraction 0.65%, molar ratio of ethanol to oleic acid 2:1, immobilized lipase particles 150 mg, phosphate buffer pH 7.0 and temperature 30 ^{O}C. As a result, maximum biodiesel conversion to 95.8% was obtained *via* esterification of oleic acid with ethanol, whereas the biodiesel yield could be maintained at 88.6% after LP@PE was used 15 times. This significant enhanced activity can be explained due to the considerably increased interfacial area of the Pickering emulsion droplets, which can improve the mass transfer of reactants and the accessibility of enzyme in the reaction system as can be seen in Fig. 5.[130]

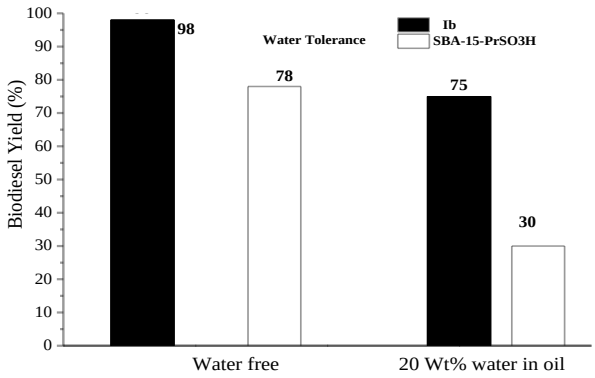

Fig. 6. Comparing water tolerance test of ethylene-PMO-PrSO$_3$H with SBA-15-PrSO$_3$H (conditions: molar ratio oil/methanol = 1/100, T = 150 ^{O}C, 6 and 3-wt% 1b and SBA-15-PrSO$_3$H catalyst, respectively), Reproduced from ref. 131 with permission from the RSC.

Recently, Karimi et al.[131] have also used PMO functionalized with sulfonic acids for biodiesel production. In their study, to optimize the hydrophobic nature of the catalyst in the vicinity of the sulfonic acid groups, they have chosen to incorporate 3-mercaptopropylmethyl dimethoxysilane into the PMO as it is well known that the presence of a methyl group bound to the same silicon atom bearing the sulfonic acid group has a remarkable shielding effect against polar molecules. In another study, it was also reported that ethylene based PMO-PrSO$_3$H catalyst is more active than phenylene based PMO-PrSO$_3$H catalyst during biodiesel formation. It has been suggested that the presence of methyl groups in the PMO may initially prevent that methanol, a polar molecule, react together with reaction by-products such as glycerine and water and subsequently

Table 1. Structural parameters and catalytic efficiencies in water-medium phenylacetylene hydration.[a]

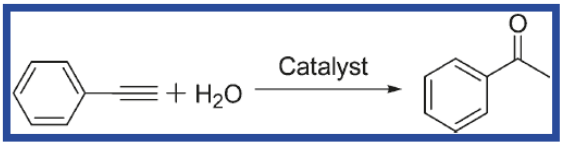

Sample	Loading	SH/SO$_3$H molar ratio	S_{BET} (m^2/g)	VP (cm^3/g)	DP (nm)	H_2SO_4 (mmol)	Yield (%)
HS-PMO(Et)	0	/	712	0.64	8	0	0
SO$_3$H-PMO(Et)	0	0	699	0.63	7.8	0	0
Au-HS/SO$_3$H-PMO(Et)-1[b]	0.10	4:3	683	0.59	7.5	0	87
Au-HS/SO$_3$H-PMO(Et)[b]	0.10	15:1	591	0.55	7.2	0	99
Au-HS/SO^{3}H-PMO(Et)-2[b]	0.10	31:1	505	0.47	6.8	0	93
Au-HS/SO^{3}H-SBA-15	0.096	/	475	0.43	7	0	90
Au/SO^{3}H-PMO(Et)	0.10	0	486	0.47	6.5	0	29
Au/HS-PMO(Et)	0.12	/	472	0.58	6.5	0	0
Au/HS-PMO(Et)	0.12	/	472	0.58	6.5	0.25	36
Au(PPh3)Clc	/	/	/	/	/	0.25	24
Au-HS/SO3H-PMO(Et)d	0.096		455	0.41	6.5	0	83

[a]Reaction conditions. [b]The Au-HS/SO$_3$HPMO(Et)-1, Au-HS/SO$_3$H-PMO(Et), and Au-HS/SO$_3$HPMO(Et)-2 catalysts were prepared from the HS-PMO(Et) with the original HS-content of 3%, 5% and 10%, respectively. [c]Reaction temperature =100 ^{O}C, reaction time = 7 h. [d] After being reused 10 times, Reproduced from re 153 with permission from ACS.

poisoning the active sulfonic acid sites. As a result an increase the catalyst stability was observed that ensure a fast and efficient mass transfer of reactants and products during reaction. In other test, results can be seen in Fig. 6, Karimi et al.[131] have compared SBA-15-PrSO_3H water tolerance with PMO-PrSO_3H showing that by adding 20-wt% water, biodiesel yield decreased by about 50% from its original value on the SBA-15-PrSO_3H.

Meanwhile, functionalized mesoporous framework with acidic or basic functional groups or metal-containing catalyst has been investigated for various catalytic applications.[20-26,151-164] For example, PMOs with different functional groups such as arene sulfonic acid ethane-silica (AS-MES), mercaptopropyl ethane-silica (Pr-SH-MES) and arene sulfonic acid SBA-15 (AS-SBA-15) were prepared. Then the catalytic reaction of these hybrid PMOs were carried out using the liquid phase acetalization reaction of heptanal by 1-butanol at 75 ^{O}C.[151] In addition, for comparison, when HY zeolite was used under same condition, it was found lower activity on HY zeolite as compared to the hybrid PMOs,[151] due to pore blocking or rapid deactivation of acid sites by water. Among all studied conducted, the higher heptanol conversion observed for arene sulfonic acid ethane-silica (AS-MES) catalyst was the result of the presence of hydrophobic organosilica framework that strengthen it's acid sites on the PMO surface.[151] Karimi et al.[155] have also demonstrated an example of Ullmann homo-coupling reaction of aryl iodides over a novel recyclable Au nanoparticles catalyst supported on benzene based PMO (Au@PMO). For comparison, Table 1 shows the structure properties of various functionalized PMO samples. *In-situ* reduction of Au^{3+} with HS-functionalized PMOs creates robust, fine Au nanoparticles and concomitantly produces a sulfonic acid moiety strongly bonded to PMOs.[153] It was found that Au nanoparticles with 1.2 nm sizes were mainly attached onto the pore surface rather than onto the outer surface of mesochannels, allowing for maximal exposure to reaction substrates and at the same time minimizing Au nanoparticle leaching.[153] The Au-HS-PMO (ethane bridged) or the Au/SO_3H-PMO (ethane bridged) produce catalyst with comparably and even higher catalytic efficiency than that of pure PMO. The developed Au-HS/SO_3H-PMO(Et) catalyst shows better efficiencies than its homogeneous counterpart in promoting water-medium alkyne hydration, intra-molecular hydroamination, styrene oxidation, and three-component coupling reactions (Table 1). This robust catalyst can easily be recycled and used repetitively at least 10 times without loss of catalytic efficiency.[153] At the same time a palladium-containing PMO with alkylimidazolium units has been reported to function as an efficient and reusable catalyst for the Suzuki–Miyaura coupling reaction of various aryl halides in water medium. Similarly ethane-PMO functionalized with a bulky N-heterocyclic carbine moiety has also been found to be efficient materials for Suzuki–Miyaura coupling reaction.[156] The Diels–Alder cycloaddition of two common dienes (cyclopentadiene and anthracene) to the double carbon–carbon bonds of an ethenylene-bridged periodic mesoporous organosilica was studied and compared to that of benzocyclobutene (Fig. 7).[158] It was found that the double bonds on the walls of an ethenylene-bridged PMO can act as dienophiles for the Diels–Alder reaction when common dienes such as cyclopentadiene and anthracene are used as feed.

Similarly, PMOs modified with surface functional groups have shown an ordered mesostructure and thermal stability similar to the parent ethylene-PMO. Ohashi et al.[159] have reported a 3-aminopropyltrimethoxysilane (3-APTMOS) grafted benzene-PMO for the Knoevenagel condensation between benzaldehyde and malononitrile. Remarkably, PMOs were found to be more active than pure mesoporous silicas. The same reaction was tested on crystal-like benzene-PMO subjected to a two-step amination process.[160] More recently, Hankari et al.[161] found that tris (3-(trimethoxysilyl)propyl)amine functionalized PMOs were more active as catalysts for the same Knoevenagel condensation reaction and for the Henry reaction of benzaldehyde and nitroethane. Different types of metal complexes have been also incorporated into the framework of PMOs to be used in heterogeneous green catalytic processes as they are easy to recover, less expensive and non-toxic, making them possible to be used on continuous reaction flow system.[20-26,162-171] For example, incorporation of arenetricarbonyl complexes within the organosilica framework of Ph-bridged PMO was successfully reported by a simple chemical vapor deposition (CVD) method.[162] Arenetricarbonyl complexes [$PhM(CO)_3$] (M = Cr, Mo) were formed by the reaction of $M(CO)_6$ with the Ph bridges, accompanied by the evolution of CO. Such metal-complex bridged PMOs could easily be employed for the development of unique catalysts such as Ir- that catalyses direct C–H borylation of arenes.[162] Moreover, it was also reported that PMOs bearing bis-(8-quinolinolato) dioxomolybdenum (VI) complexes can be employed for olefin epoxidation such as cyclooctene in the presence of tert-butyl hydroperoxide (TBHP) as reaction oxidant.[171] It is also reported that all MoO_2-PMOs catalysts are active for the epoxidation of cyclooctene with

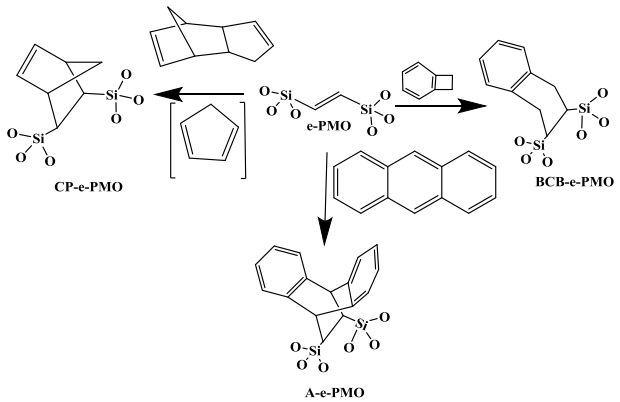

Fig. 7. Formation of three surface Diels–Alder adducts by reaction of a dienophile (e-PMO) and three different dienes (dicyclopentadiene, benzocyclobutene and anthracene). These units represent a fragment of the organosilica wall and so the oxygens are embedded in the pore wall, Reproduced from ref. 158 with permission from the RSC.

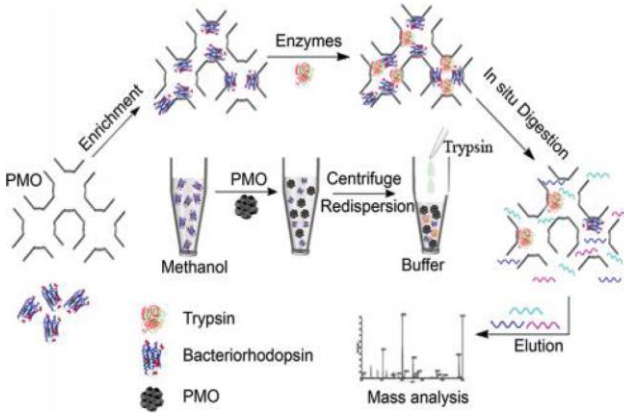

Fig. 8. Schematic Illustration of the PMO-assisted strategy employed for efficient identification of hydrophobic membrane proteins, Reproduced from ref 174 with permission from ACS.

nearly 100% of selectivity to epoxycyclooctane. MoO_2Q_2@PMO-6% has shown the highest conversion of 48.8% after 8 h reaction as a result of its uniform spherical morphology, well defined order and massive mesopores embedded in the framework that facilitate the mass transfer of reactant and products. It was found that catalyst is stable instead of significance leaching.[171] On the other hand, well-organized metal-tetrakis(carboxyphenyl)porphyrin (Metal = Fe, Cu, Sn) bridged PMOs (M-TCPP-PMO) with high surface area were synthesized and used as catalyst for the Baeyer-Villiger oxidation of ketones.[168] Among the catalysts, the high catalytic activity observed for Fe-TCPP-PMO over Cu-TCPP-PMO and Sn-TCPP-PMO was attributed to the high Fe-porphyrin valence on the pore wall of organosilica framework along with cyclohexanone, suggesting that Fe-TCPP-PMO could be a promising and efficient catalyst for the Baeyer-Villiger oxidation of ketones to esters using O_2 as the oxidant.[168] Importantly, no leaching was observed when vanadyl Schiff base complexes were successfully employed to catalyze efficiently the cyanosilylation of carbonyl groups.[163] Bridge organophosphine complexes functionalized PMOs have been also reported as catalysts for a great variety of organic reactions (such as Suzuki cross-coupling, Diels–Alder) and different bis- and tris-silylated phosphine complex precursors in the presence of various different metals.[164,166,169-171] These materials have shown similar/very comparable activities to the homogeneous complexes and could easily be recycled few times due to their resistance to leaching. For example, co-condensed PMOs were found to be more active than similar grafted materials because the grafting method could lead to pore blockage and leach out catalyst during washing time.[4,5,15] Recently, Zhang et al.[46] has reported that immobilization of a site-isolated organopalladium functionality and chiral organoruthenium functionality on a single PMO was used for synthesis of chiral biaryl alcohols by cascade asymmetric transfer hydrogenation and Suzuki cross-coupling of haloacetophenones and arylboronic acids.[46]

3.2 Enzyme immobilization

PMOs are also being used as host materials for adsorption/immobilization of biomolecules.[20-26,132-148] Recently a hydrophobic benzene based PMO material has shown better adsorption affinity to lysozyme when compared with a ethane-based PMOs.[132] It is known that ordered mesoporous structured materials with rather narrow pore sizes are excellent supports for lipase immobilization when the surface is more hydrophobic. This is not possible via grafting with organic functional groups because post-grafting method is not only highly associated with leaching out organic functional groups but also with pore blocking and heterogeneous distribution of organic functional groups. What happens is that the soft interaction of the protein with the hydrophobic ungrafted surface *via* post-grafting method results in a much lesser activity loss.[133] It was found that horseradish peroxidase (HRP) can also be immobilized on PMOs. Studies suggested that the organic-inorganic nature of framework gives them superior properties when used as supports, as could also protect immobilized enzyme and enhance its enzymatic activity.[132-148] Recently a monodisperse nanosize Co_3O_4 core-mesoporous organosilica shell nanosphere was synthesized by cooperative self-assembly of organosilica precursor and surfactant molecules on the Co_3O_4 nanoparticles surface. Co_3O_4/PMO core–shell structured nanospheres are highly promising to the adsorption of microperoxidase-11(MP-11).[146] More excitingly, it was found that core-shell nanospheres structures have a positive effect on the catalytic reaction of Microperoxidase-11 (MP-11). Lu et al.[147] have coated and encapsulated barium ferrite $BaFe_{12}O_{19}$ (BaFeO) nanoparticles (with a size of 100 nm) inside PMO host material, forming magnetic PMO nanoparticles with a relatively high magnetic response (25 emu g^{-1}) and a high loading capacity of 1.315 mg per mg towards enzyme mixture. This study further demonstrated that MHPMO materials exhibited enhanced cellulose tissue penetration behaviour under external magnetic field.[147]

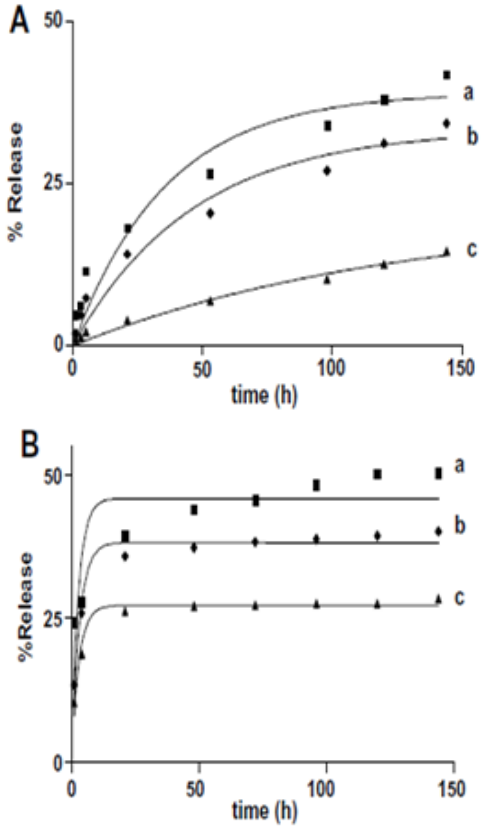

Fig. 9. Release kinetics of TC loaded on PMS-SS (a), PMO-SS (b), PMO-HS (c) in SBF solution (A) and PB solution (B) respectively. Symbols: experimental data; solid lines: fitting results by first order mass transfer model, Reproduced from ref 150 with permission from Elsevier.

3.3 Refolding of proteins and protein membrane

Many studies have examined applications of PMOs in the field of adsorption and delivery of drugs, genes and enzymes under a range of internal/external stimuli, such as temperature, redox, pH, light, magnetism and ultrasound,[20-26,172-174] whereas an interesting application of PMOs for protein refolding has not been sufficiently explored yet.[173] Feng et al.[172] reported that ethylene-bridged PMOs with pore size 4.8 nm effectively entrap unfolded proteins and assist refolding by controlled release into the refolding buffer. Hen egg white lysozyme (molecular dimensions of 1.9 × 2.5 × 4.3 nm^3) was used as a model protein to demonstrate the new method of protein refolding and how the organized mesopores of PMO can effectively entrap denatured proteins and minimize protein aggregation.[172] This study has suggested that ethane-PMOs with surface silanols can interact with hydrophobic parts of the protein and the exposed charge of amino acid residues, respectively, which contributes to adsorption of the protein. This has also shown that poly(ethyleneglycol) (PEG)-triggered continuous release of entrapped denatured lysozyme that allows high yield refolding with high cumulative protein concentrations. This new method

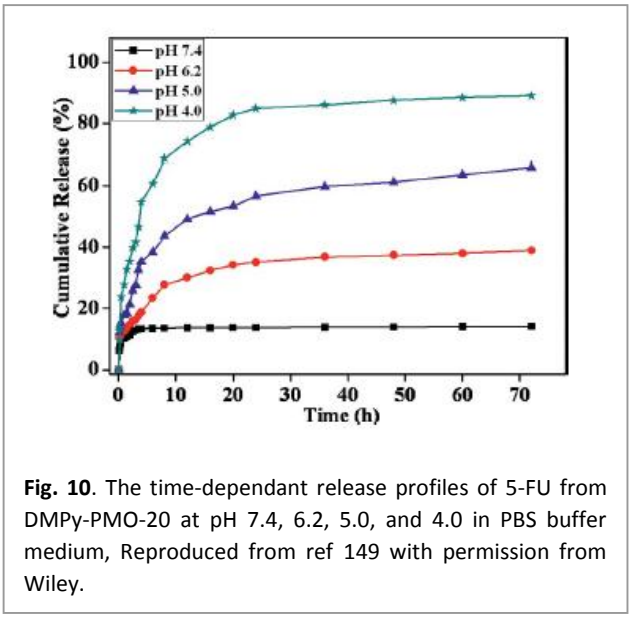

Fig. 10. The time-dependant release profiles of 5-FU from DMPy-PMO-20 at pH 7.4, 6.2, 5.0, and 4.0 in PBS buffer medium, Reproduced from ref 149 with permission from Wiley.

enhances the oxidative refolding of lysozyme (e.g., over 80% refolding yield at about 0.6 mg/mL).[172] Moreover, the PEG molecules can form strong hydrogen bonds with the Si-OH groups. It was found that when comparing with SBA-15 samples the release is much more hindered in comparison to the PMO samples that give the best release velocity results. Gan et al.[174] have developed a versatile protocol shown in Fig. 9 for large-scale characterization of membrane proteins using a three-dimensional PMO-based membrane nanodevice for detecting

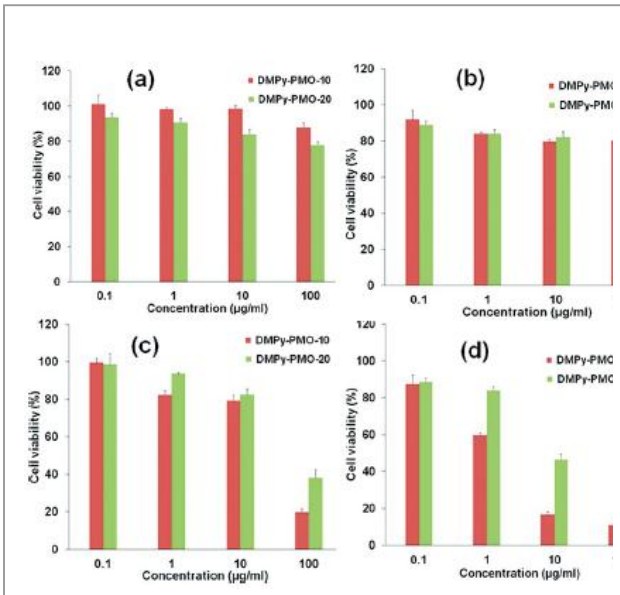

Fig. 11. The *in-vitro* cytotoxicity of DMPy-PMOs with two different particle sizes with various functional-group contents against MCF-7 cells at pH 7.4 and 6.1. Cytotoxicity profiles of blank DMPy-PMO particles (a and b) and 5-FU-loaded DMPy-PMO particles (c and d) at concentrations of 0.1, 1, 10, and 100 μgmL^{-1} at pH 7.4 (a and b) and 6.1 (c and d), Reproduced from ref 149 with permission from Wiley.

proteins at a low concentration. This study shows an effective method to the digestion of complex samples indicating its potential application in membrane proteome analysis.

3.4 Biomedical applications (drug delivery and biomedicine)

Application of PMOs also largely depends on how and what kind of organic functional groups are integrated into the framework of PMO.[20-28,157] Lu and co-workers have reported the effects of morphology, wall composition and the use of different buffer solutions on drug delivery application and how these properties have played an important role in controlling both adsorption capacity and the release rate of drug molecules.[150] In this way the authors found that hybrid PMO materials with hydrophobic ethylene group on their wall framework possess higher loading capacities and significantly lower release rate of tetracycline (TC) than pure PMS materials because of their stronger hydrophobic–hydrophobic van de Waals attraction forces with tetracycline molecules. Two kinds of release medium that were used in this study i.e., simulated body fluid (SBF) solution (pH 7.4) and phosphate buffer (PB) solution (pH 1.5), revealed very different release profiles. A slower delivery rate was observed when SBF solution was used that can be attributed to the different ionic interactions between the guest molecule and the host material in the two different pH solutions. Overall, hollow PMO shows the lowest release rate and the highest loading amount compared to the other two materials (Fig. 9).[150] Recently, it has been reported that PMO with hetero-aromatic pyridine ring containing two N–H sites showed few advantages including good mesostructural order, selective nucleobase-recognition properties, and stimuli-responsive site-specific delivery of anticancer agents to cancer tissues into a single entity.[149] Fig. 10 shows the time-dependant release profiles of 5-FU from DMPy-PMO-20 (N,N/-disilylated pyridine-bridged PMOs) at pH 7.4, 6.2, 5.0, and 4.0 in PBS buffer medium. From the result it can be assumed that this hybrid PMO chemo-sensor showed an intrinsic selective recognition for a nucleobase, such asthymidine, due to multipoint hydrogen-bonding interactions that comprises of suitable arrayed receptor sites loaded into the rigid silica framework. An *in-vitro* cytotoxicity test suggested the good biocompatibility of designed chemo-sensor materials (Fig. 11) and, therefore, they could be promising potential candidates for the delivery of a range of therapeutic agents. In addition, confocal laser scanning microscopy (CLSM) confirmed that the material can be internalized effectively by cancer cells (MCF-7 cells).[149]

In 2014, Wang et al.[157] designed molecularly organized hollow PMO nanoparticles (HMONs) with a variety of silsesquioxanes bridged to demonstrate how these materials can improve therapeutic performance and enhance the biological effects beneficial for biomedicine application. Fig. 12 shows their strategy which was adopted using a generic

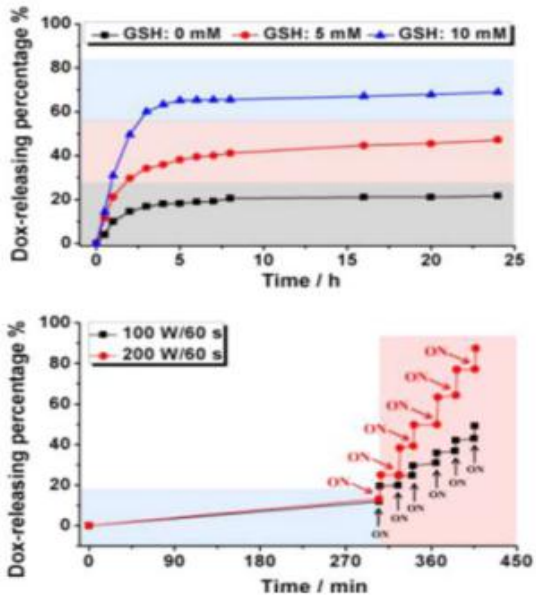

Fig. 13. (Top) Cumulative Dox-releasing percentages at the glutathione (GSH) concentrations of 0, 5, and 10 mM in PBS solutions. (bottom) HIFU-triggered Dox-releasing profiles at different power densities (100 and 200 W/cm², 60 s irradiation), Reproduced from ref 157 with permission from ACS.

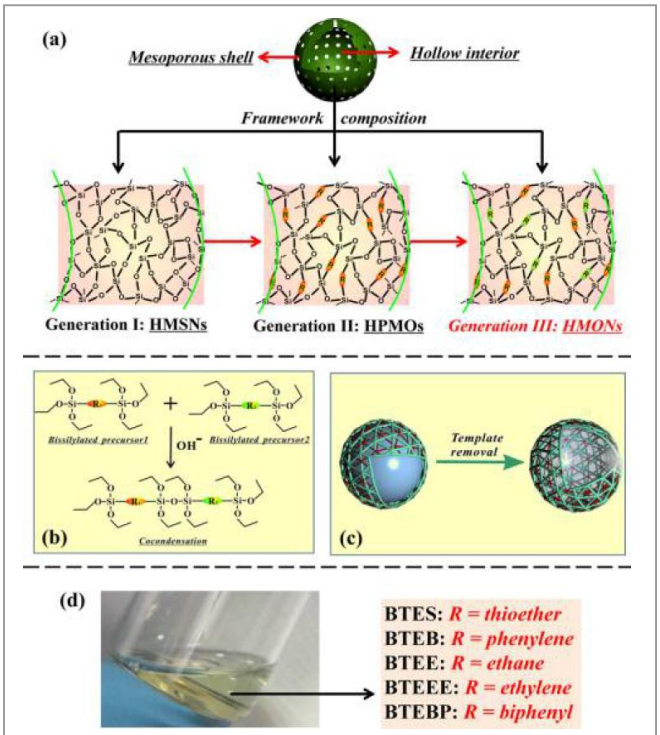

Fig. 12. (a) Illustration of the evolution of three generations of silica-based hollow mesoporous capsules classified in terms of chemical composition of the shell. (b) The chemical homology principle for constructing the hybrid silsesquioxane framework of HMONs. (c) The scheme of templating method to fabricate dual-functionalized HMONs (R_1: thioether, R_2: phenylene). (d) Photographic image of homogeneous solution of up to five bissilylated organosilica precursors miscible with each other, including BTES (R_1), BTEB (R_2), BTEEE (R_3), BTEE (R_4), and BTEBP (R_5), Reproduced from ref 157 with permission from ACS.

intelligent framework-hybridization approach for biomedicine.[157] They found that the hybridization of physiologically active thioether groups with triple distinctive disulphide bonds present in the framework structure can provide HMONs with unique intrinsic reducing/ acidic- and as such external high intensity focused ultrasound (HIFU)-responsive drug-releasing performances, improved biological effects (e.g., lowered hemolytic effect and improved histocompatibility), and enhanced ultrasonography behavior.[157] The doxorubicin-loaded HMONs with concurrent thioether and phenylene hybridization exhibit drastically enhanced therapeutic efficiency against cancer growth and metastasis, as demonstrated both *in vitro* and *in vivo*. This study showed that that the triple disulfide bonds in a thioether group within the framework are highly responsive to reducing environments to quickly trigger the releasing of loaded guest molecules. The releasing patterns of Dox-loaded HMONs in Fig. 13 were studied at different GSH (0, 5, and 10 mM) concentrations in a Phosphate buffer solution (PBS). The release of Dox in pure PBS showed slow and sustained profile with only 21.8% releasing percentage in 24 h whereas the addition of GSH has increased releasing percentage to 47.2% and 69.0% at the GSH concentrations of 5 and 10 mM, respectively, in 24 h. It can be concluded that in this hybrid system, after the reduction and subsequent cleavage of disulfide bonds within the thioether functional groups, the initially established π–π supramolecular stacking and hydrophobic–hydrophobic interaction between the framework and the aromatic Dox molecules can be broken up, leading to the substantially increased drug-releasing rates.[157]

Fig. 14 shows also the therapeutic efficiency of HMONs for *in vivo* anticancer drug delivery/chemotherapy assessed on 4T1 orthotopic mammary tumor spontaneous metastasis xenograft. It is suggested that the tumoridical efficiency of Dox loaded HMONs is significantly higher than free Dox (Fig. 14a). The tumor volume (Fig. 14b) and weight (Fig. 14c) were found to be reduced for Dox-HMONs treated samples compared with those of free Dox group. In addition, the high tumoridical efficiency by Dox-HMONs could be supported by the fact that significantly enhanced tumor destruction and cell apoptosis of Dox-HMONs group has been reported by pathological hematoxylin and eosin stain (H&E) analysis and TUNEL staining.[157] It could be suggested that one of the studies that shows the delivery of Dox mediated by HMONs can bring substantially enhanced destruction/apoptosis effects against tumors, significantly inhibited tumor metastasis and decreased angiogenesis.[157]

On another interesting work, Durand et al.[140] have described the synthesis of new mixed PMO nanoparticles (MPMO NPs) as a result of the co-condensation product of a tetra-trialkoxysilylated two photon photosensitizer with bis-(triethoxysilyl)phenylene or ethylene. The MPMO NPs are found to be very efficient for anti-cancer drug delivery combined with two-photon therapy in MCF-7 breast cancer cells, leading down to 76% cancer cell death. This study has used a series of PMOs with different conditions and found that MPMO NPs are very promising for nanomedicine applications. Same group has reported porphyrin-functionalized ethylene bridged PMO nanoparticles (denoted at EP-NPs) for two-photon imaging of breast cancer cells and drug delivery applications.[137] The two-photon imaging capacity of the EP-NPs assessed in cancer cells is shown in Fig. 15. Finding from this study has demonstrated the suitability of porphyrin-functionalized mesoporous organosilica nanoparticles for two-photon imaging. In addition to two-photon fluorescence study, EP NPs were incubated with MCF-7 for 72 h and found to be remarkably efficient to cause cell death as only 25% of cancer cells survived at a concentration of EP NPs of only 1 μg mL^{-1} (Fig. 16).

3.5 Magnetic PMOs

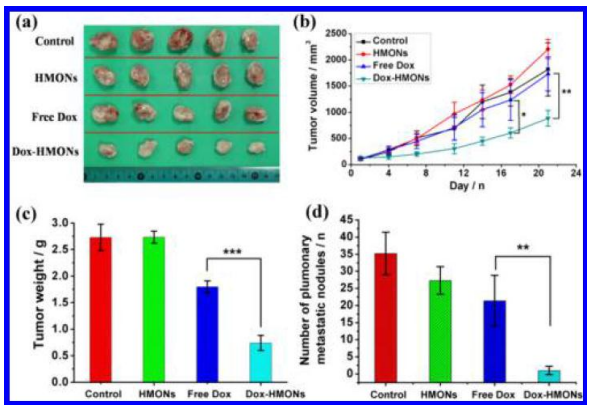

Fig. 14. (a) Photographic images of tumors after different treatments. (b) The tumour volume changes as a function of time after different treatments (n = 5). (c) The tumor weights at the end of treatment. (d) The number of pulmonary metastatic nodules in lungs of mice after different treatments. **P < 0.01, ***P < 0.001, Reproduced from ref 157 with permission from ACS.

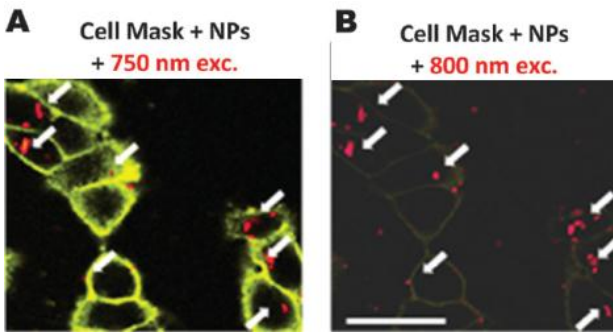

Fig. 15. Cell membranes were stained with Cell Mask TM Orange Plasma Membrane, EP NPs were incubated and irradiated at 750 (A) and 800 nm (B). Arrows indicate NPs in cells. Scale bar is 10 mm, Reproduced from Ref. 137 with permission from the RSC.

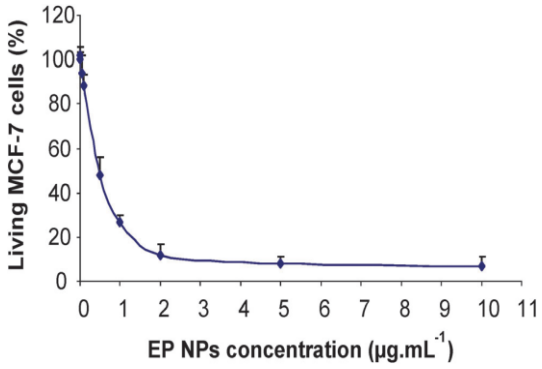

Fig. 16. Doxorubicin delivery in MCF-7 cancer cells *via* EP NPs, Reproduced from ref. 137 with permission from the RSC.

The modification or coating of magnetic nanoparticles with silica or polymers has been extensively studied for biomedical fields including targeted drug delivery systems, magnetic resonance imaging (MRI) contrast agents, protein separations, cell sorting, and immunoassays.[177-183] Recently, Lu and his co-workers[182] have demonstrated a novel class of magnetic composite PMO hollow spheres and Fe_3O_4 nanocrystals. The high saturation magnetization ensures (Fig. 17) that these functional mesoporous hollow spheres can be used as a very efficient protocol to targeted drug delivery and also be assisted by magnetic fields. In addition, the principle demonstrated in this work may also allow core/shell synthesis of nanocrystals or semiconductor quantum dots (e.g., CdSe, Au) encapsulated in hollow silica spheres, which may lead to many promising applications in enzyme immobilization, cancer therapies, and MRI contrast agents but toxicity studies of these suggested quantum dots have to be ensured for before practical applications.

3.6 Chromatography

Chromatography is currently the most commonly applied technique for separating and analysing multi-component mixtures.[20-26,184-195] In this field, silica is commonly used as stationary phase whereas more than 60% of all HPLC separations are carried out under reversed phase (RP)

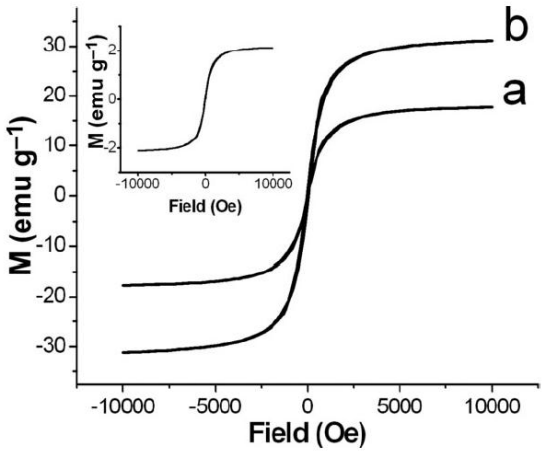

Fig. 17. Field-dependent magnetization curves at 300 K of a) PMO–MHS2, and b) PMO–MHS4. Inset: curve for PMO–MHS1, Reproduced from ref 182 with permission from Wiley.

conditions.[184-186] The surface modification of well-defined silica beads with T-silyl functionalized organic systems is the major route for creating phases for reversed phase liquid chromatography (RPLC). In this context, the presence of organic and inorganic functions in PMO framework can tune the polarity of the PMOs and as such it could be easier to design a whole broad spectrum of stationary phases which can be located in every desired place between the extremes of a normal (very polar pure silica phase) and a reversed HPLC phase (very non-polar phase consisted of silica capped with organic hydrophobic group). Corriu et al.[186] have shown that PMOs with high surface areas along with particle size less than 1 µm have been used as suitable stationary phases in HPLC for separating different standard reference materials (SRMs) containing polycyclic aromatic hydrocarbons (Fig. 18). It was found that the spherical phenylene-PMOs (0.16 silanol groups per nm^2) were able to cleanly separate all three test mixtures (BHT, Sorbic acid, and Aspartame), despite the wide range of polarities of the individual analyte when compared with a normal phase Nucleosil50-10 (Nucleosil50–10 contains a significantly higher concentration of 4.82 silanol groups per nm2).[187] Phenyl-functionalized ethane-bridge PMOs have shown better separation capacity of polycyclic aromatic hydrocarbons than C8-immobilized pure mesoporous silicas. The chiral PMOs with trans-(1R,2R)-diaminocyclohexane group have higher enantioselectivity for nine amino acids over other chiral silica based stationary phases and these chiral PMOs with trans-(1R,2R)-bis-(ureido)-cyclohexane also provide baseline separation of (R/S)-1,1/-bi-2-naphthol enantiomers at high sample loading and high flow rate.[194,195] Recently, Ide et al.[185] have reported the synthesis of a novel cyclic multifunctional organosilane-based PMO with 2 µm size particles. The PMO spherical silica particles are not only

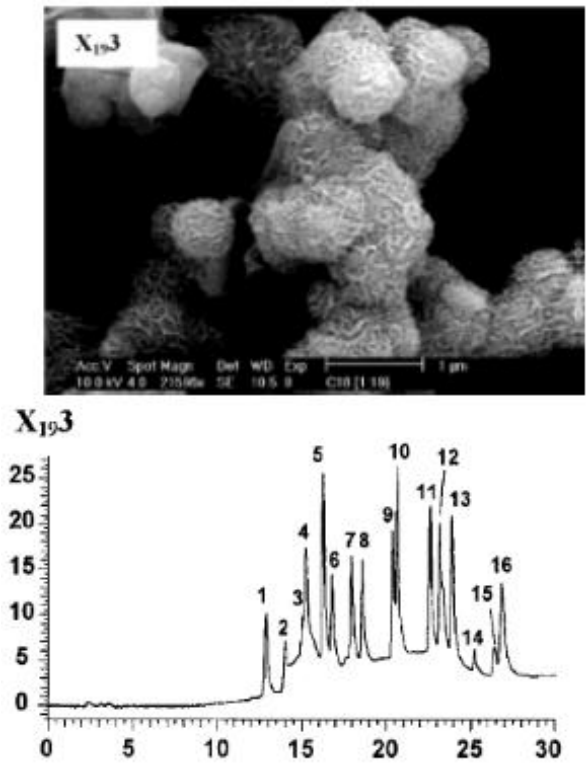

Fig. 18. (Top) SEM image of $X_{19}3$ and (Bottom) Separation of the 16 priority pollutant polycyclic aromatic hydrocarbons (SRM1647c: 1: naphthalene, 2: acenaphthylene, 3: acenaphthene, 4: fluorene, 5: phenanthrene, 6: anthracene, 7: fluoranthene, 8: pyrene, 9: benzo[a]anthracene, 10: chrysene, 11: benzo[b]fluoranthene, 12: benzo[k]fluoranthene, 13: benzo[a]- pyrene, 14: dibenz[a,h]anthracene, 15: benzo[ghi]perylene, 16: indeno[1,2,3- cd]pyrene) on the mesoporous stationary phases $X_{19}3$, Reproduced from ref 186 with permission from Wiley.

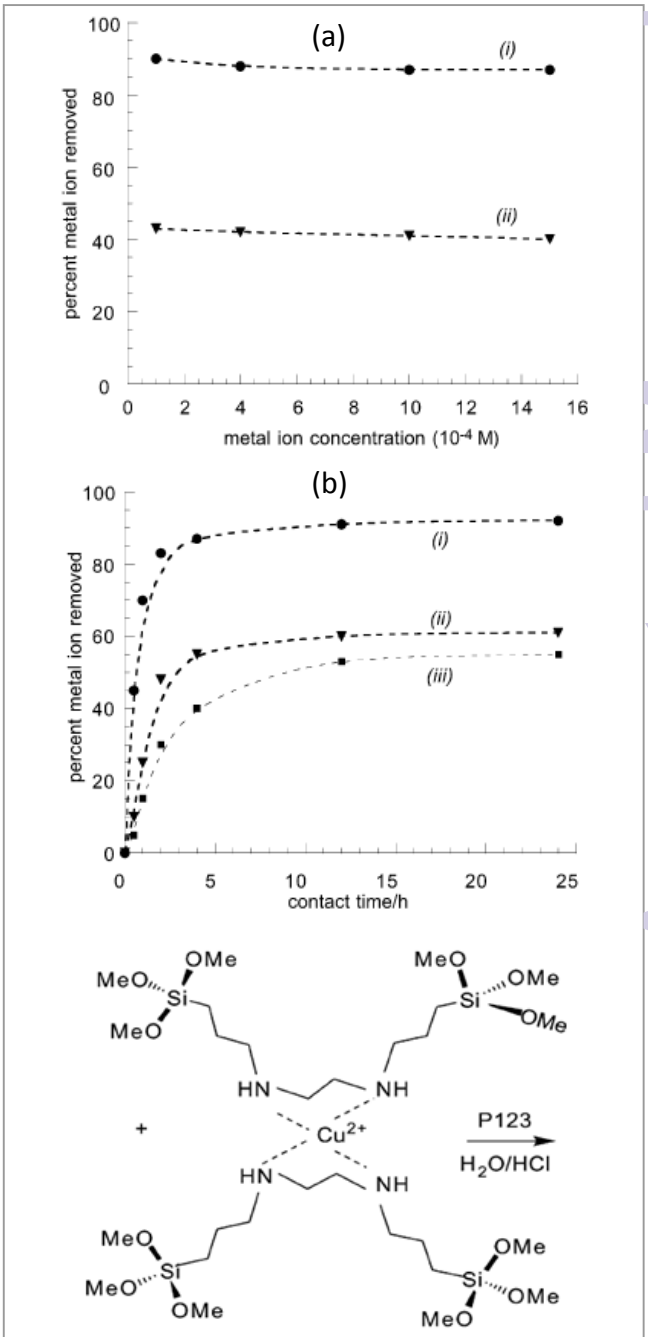

Fig. 19. (a) Cu^{2+} and Zn^{2+} uptake by EBPEDS-0.2 (Solutions equimolar in Cu^{2+} and Zn^{2+}). Samples are ethanol/HCl extracted, and rinsed with dilute NH_4OH and water prior to equilibration for 4 h. (b) Percent copper absorbed from aqueous solutions (10^{-3} mol dm^{-3}) of the corresponding acetate versus contact time for (i, iii) Cu^{2+}; (ii) Zn^{2+}; (i, ii) samples rinsed with NH_4OH and water prior to uptake experiment; (iii) sample in protonated form. (c) the synthesis of bridge-bonded bifunctional PMO towards metal on, Reproduced from ref 197 with permission from ACS.

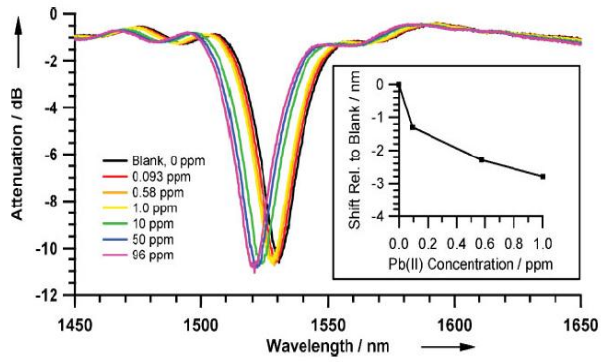

Fig. 20. Optical response of the PMO-coated LPG to aqueous DMSO solutions (RI¼1.402) of Pb (II) of increasing concentration as observed with the LPG attenuation spectra and by the shift in the resonant peak position as a function of solution concentration (inset), Reproduced from ref 207 with permission from Wiley.

hydrolytically stable stationary phase in reversed phase HPLC but also proved to be both highly retentive and stable in a pH range from 1.75 to 12 and up to 150 ^{O}C in 60 v% water, indicated the high stability of the backbone and the functionalities of the material.

3.7 Environmental (inorganic and organic pollutants)

PMOs can play also very significant role for water treatment process and environmental applications since functionalized PMOs could be in the range of materials with targeted functional groups that could be used efficiently and according to target pollutants.[20-26,196-201] For example, ethylenediamine ligand of N,N/-bis[3-(trimethoxysilyl)propyl]-ethylenediamine an important part of PMO framework enables to bind metals directly within the framework walls of PMOs (Fig. 19).[197] On the other hand, crystalline PMOs with densely packed pyridine units (v-Py–PMO) within the framework were found to be accessible for reversible protonation and Cu^{2+} adsorption.[198] In comparison, pyridine groups containing PMOs show higher adsorption capacity for Cu^{2+} whereas similar PMOs with

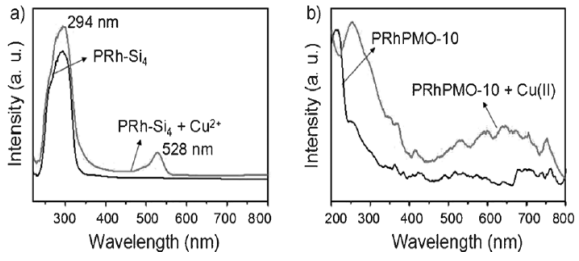

Fig. 21. (a) UV/Vis spectra of PRh-Si4 in THF before (PRh-Si4) and after (PRh-Si4+Cu^{2+}) the addition of copper ions. (b) UV/Vis diffuse reflectance spectra of PRhPMO-10 and Cu2+-chelated PRhPMO-10, Reproduced from ref 212 with permission from Wiley.

divinylbenzene group (Si–C_2H_2–C_6H_4–C_2H_2–Si) showed little Cu^{2+} adsorption capacity.[170] The adsorption capacity, 2.4 mmol g^{-1} at 0.018 M Cu^{2+}, indicated that 71% of the total pyridine groups in v-Py–PMO are bound with Cu^{2+}. The adsorbed Cu^{2+} was almost completely removed by washing with water while preserving the PMO structure. On another example, PMOs functionalized with isocyanurate groups showed an adsorption capacity of 1.8 g of Hg^{2+} per g of adsorbent[199] whereas disulfide groups functionalized PMOs have an adsorption capacity of the same material of about 864 mg g^{-1} of Hg^{2+} ions, demonstrating its potential use as an adsorbent for adsorption of heavy metal ions from wastewater. Recently a synthesized PMO containing the hetero-aromatic pyridine ring and two N–H sites in the framework showed adsorption capacity of 0.95 mmolg^{-1} for Cu^{2+}.[149] The enhanced adsorption capacity of functionalized PMOs was due to the presence of electron-rich pyridine and N–H sites. Beside these, depending on the nature of organic ligands in the framework of PMOs, a broad wide range of PMOs with various organic groups have been developed and employed for studying the adsorption capacity of heavy metal ions including Cu^{2+}, Cd^{2+}, Cr^{3+}, Hg^{2+}, Mn^{2+}, Fe^{3+}, Fe^{2+}, Co^{2+}, Ni^{2+}, Zn^{2+}, Pb^{2+}, Pd^{2+}, Pt^{2+}, Au^{3+}.[20-26,196-206] Recently, PMOs with

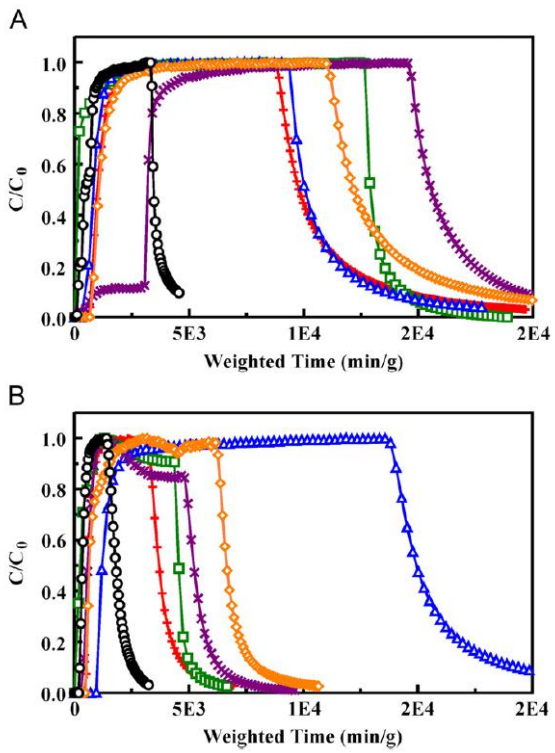

Fig. 22. Ammonia micro breakthrough curves for organosilicates under (A) dry and (B) humid RH(80%RH) conditions. E50assynthesized (X), at pH 7(diamond), and pH 9 (+) is compared to BPL/Zn/TEDA (circle), E50-A (square), and E50-I functionalized (triangle) materials. Overall, the material grafted with isocyanate functional groups (E50-I) exhibited the best ammonia removal capabilities, Reproduced from Ref 215 with permission from Elsevier.

benzene and ethane groups were also used for the selective adsorption of organic pollutants including 2,4,6-trinitrotoluene (TNT), cresol, 4-nitrophenol, phenol, 1,3,5-hexahydro-1,3,5-trinitrohydrazine and benzene.[203-206] It was found that the hydrophobic nature of the PMOs themselves imparted good sorption properties towards these compounds (up to 500 mg g^{-1}). Depending on the nature of functional groups in the PMO framework, these PMOs could be used for adsorption of toxic oxyanions, rare earth metal ions, radionuclides, dyes, pesticides and pharmaceuticals.

3.8 Sensors

A sensor is a device that detects and responds to some type of input from the physical environment. The specific input could be light, heat, motion, moisture, pressure, or any one of a great number of other environmental phenomena. The output is generally a signal that is converted to human-readable display at the sensor location or transmitted electronically over a network for reading or further processing.[20-26,207-112] PMOs with organized pores have attracted attention as potential sensor devices because mesoporous channels allow incorporation of guest compounds into the mesoporous framework and might possess suitable interaction centres in their interior/pore walls structures, which may then induce a signal, i.e. a property change that can be detected. Recently, Crudden et al.[207] have reported PMO coating as the key component in a sensitive and tunable fiber-optic evanescent wave sensor for the ppb-level detection of Pb (II) (Fig. 20). Authors have suggested the possibility of extending this method to detect industrially relevant metal contaminants including mercury and nickel. Importantly, they also stressed that such chemically selective, processable, and versatile mesoporous organosilica films will be of great interest to research as have the potential to develop micro-resonators and other sensitive optical and evanescent field devices. Detection of organic explosive such as p-nitrophenol, p-cresol, 2,4,6-trinitrotoluene and RDX (1,3,5-trinitroperhydro-1,3,5- triazine) using porphyrin embedded nanoporous organosilicas has recently been successfully reported.[210] Ha et al.[209] used rare-earth ions (Eu^{3+},Tb^{3+} and Tm^{3+}) to dope PMO monoliths which have shown red-, green- and blue-emissions upon UV irradiation with characteristic emission peaks, that have also been suggested for UV-sensors. In 2015, Qiu et al.[212] have demonstrated pentyl-linked bis(rhodamine)-derived tetra-siloxane (PRh-Si4) based highly ordered PRh-bridged periodic mesoporous organosilicas (PRhPMOs) for ratiometric fluorescent nanosensors for Copper (II). Fig. 21 shows the UV/Vis spectra of PRh-Si4 and PRhPMO-10 before and after the addition of copper ions. It is reported that a band centred at λ=294 nm and a band at 528 nm emerged for PRh-Si4 upon the addition of Cu^{2+}, which is the result of the ring opening of the five-membered nitrogen-containing heterocycle in the PRh unit after complexation whereas the π–π* electronic-transition occurred due to the aromatic rings in the framework. A broad red shifted peak at λ=600 nm was found for Cu^{2+}-chelated complex PRhPMO-10 due to the formation of J-aggregates of the PRh units in PRhPMO-10. The presented results suggested the possibility to use PRhPMO ratio metric fluorescent chemosensors for Cu^{2+}.[212]

3.9 Gas (adsorption/separation) and hydrogen storage

Gas separation/adsorption/storage processes are very important and being explored in terms of academic and practical environmental and industrial discharge.[212-118] Hence, ethane-bridged PMO materials have been used for the adsorption of various gases including sulfur dioxide, cyanogen chloride, ammonia and octane (Fig. 22). Systematic studies on the adsorption of hydrogen gas and its interactions with the various bridged organic functional groups (ethylene-, ethane-, phenylene- and biphenylene)-based PMO materials have been explored, whereas it was found that ordered phenyl-PMOs can adsorb more hydrogen than the ethane-PMOs.[216] On the other hand, phenyl-PMO was used to remove highly toxic polycyclic hydrocarbons from aqueous solutions[217-219] whereas functionalized amine-bridged PMO materials are found to be efficient for CO_2 adsorption. The low-temperature interaction of CO with the hybrid surface of crystalline phenyl PMOs has been proven as a result of the double interaction that arises from dispersive interaction between the CO molecule and the polarizable benzene ring.[220] Very recently, ordered and disordered phenylene-PMOs have shown properties as materials for H_2 storage.[221] These materials exhibit a reversible hydrogen excess surface adsorption capacity up to 2.10 wt% at 6 MPa and 77 K. DFT calculations that were performed to define the binding strength of H_2 with the pore walls found an interaction energy value of 0.55 Kcal mol^{-1}, higher than the corresponding interaction energy value of hydrogen with a single benzene molecule.[221]

3.10 Light harvesting (LH) materials based PMOs and photocatalysis

The use of energy harvesting materials have received vast interest since energy based applications as photocatalysts, photovoltaic devices, and light-emitting devices will play important role in the future energy sectors. Recently, the light-harvesting effects of PMOs that contain a high density of aromatic bridges has been explored successfully since aromatic chromophores could easily be located in the framework and meso-channels of PMOs, enabling the rational design of excited energy transfer from donors in the framework to acceptors in the meso-channels. The tuning of PMO pore walls with different photoactive species enables

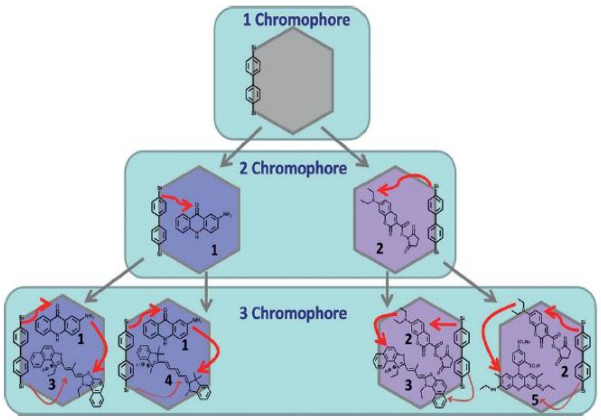

Fig. 23. Schematic diagram of different chromophore systems, which were built by loading of extracted biphenyl-bridged PMO with different dye molecules. The red arrows show the route of the energy transfer from donors to acceptors, Reproduced from ref 233 with permission from Wiley.

Table 2. Summary of the synthesized materials with the energy transfer efficiency from chromophore 1 to chromophore 2 (E_{12}), from chromophore 2 to chromophore 3 (E_{23}), and of two-step-FRET from chromophore 1 through chromophore 2 to chromophore 3 (E_{123}).[a],233

Chr1	Chr2	Chr3	Emission Maxima[b]	E_{12} (%)	E_{23} (%)	E_{123} (%)
Donors	Acceptors					
Biphenyl-PMO	-	-	374	-	-	-
Biphenyl-PMO	Aminocridone	-	519	95	-	-
Biphenyl-PMO	diethylaminocouramin	-	477	91	-	-
Donors	Mediators	Acceptors				
Biphenyl-PMO	Aminocridone	Dibenzothiacarbocyanine	630	95	84	80
Biphenyl-PMO	Aminocridone	Indocarbocyanine	692	95	78	74
Biphenyl-PMO	diethylaminocouramin	Dibenzothiacarbocyanine	634	91	80	73
Biphenyl-PMO	diethylaminocouramin	Sulforodamine	567	91	76	69

[a] The wavelength of the emission maxima of acceptors and the values of the energy transfer efficiency are represented for samples with maximal concentration of the acceptors before the onset of emission quenching of the acceptors occurs. Chr=Chromophore. [b] Emission maxima of the last chromophore.

the energy transfer between two species within a single material.[22,222-233] Recently, biphenyl-bridged hexagonal PMO with a crystal-like pore wall structure was used as a template to build two- and three-chromophore systems with a light-harvesting function as shown in Fig. 23.[223] Table 2 shows the summary of the synthesized materials with the energy transfer efficiency. Two-chromophore systems with an additional dye in the pores show that excitation energy absorbed by biphenyl groups (donors) can be transferred to either aminoacridone or diethylaminocoumarin (acceptors) through FRET with high transfer efficiencies of 91–95%.[223] On the other hand, light-harvesting three-chromophore systems were prepared by incorporation of two types of dye molecules into biphenyl-bridged PMO, in which each dye in the mesochannels acts as a mediator and acceptor. The consecutive two-step-FRET from biphenyl groups to acceptors, conveyed by mediators is observed with high energy-transfer efficiencies from 70 to 80% at very low concentrations of each dye. Results have suggested that the organized pores of PMO contain enabled mediator/acceptor pairs that can be arranged in close mutual proximity for an efficient direct energy transfer.[223] Inagaki et al.[227] have also reported that the increasing amount of light harvesting coumarin doped-PMOs weakened fluorescence emission of biphenyl group whereas the blue emission of coumarin dye strengthened it. The energy transfer efficiency estimated from the fluorescence quenching of the biphenyl bridge is close to 100%, even at a low coumarin concentration of 0.80 mol% to the 4,40-biphenylylene (Bph) bridged unit (one coumarin molecule per 125 Bph units).[227] As shown in Fig. 24, the fine-tuning of the emission colors over a wide range of the

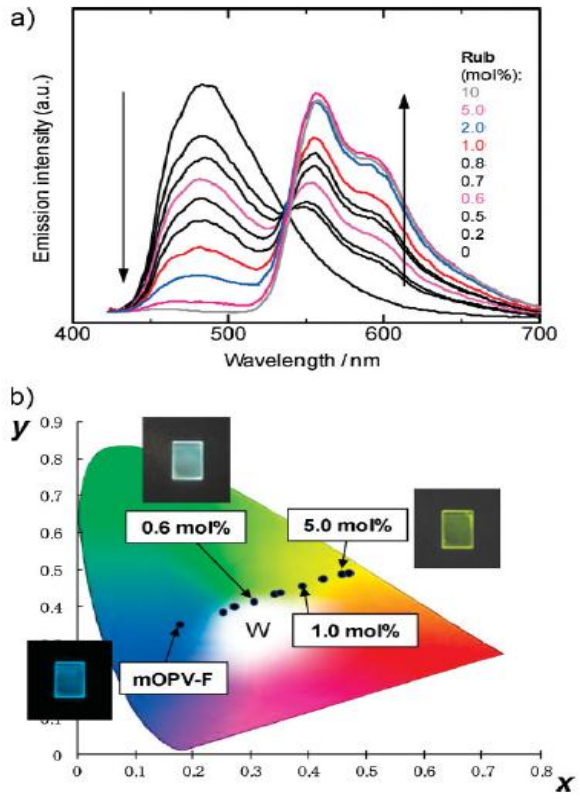

Fig. 24. (a) Fluorescence spectra of mOPV-F films doped with Rub (0–10 mol % ratio to the OPV unit). (b) Emission colours in the CIE 1931 chromaticity diagram calculated from the fluorescence spectra of Ru-doped mOPV-F films and the photographs of the films under 365 nm UV irradiation, Reproduced from ref 229 with permission from Wiley.

visible spectrum including a white light emission was reported for fluorescence dyes doped-PMO, indicating possible luminescence applications including LEDs and fluorescence sensing.[229] Evaporation-induced self-assembled transparent and visible light-harvesting acridone-bridged containing PMO films (from non-methylated and N-methylated acridonebridged bis-triethoxysilane precursors) have shown that non-methylated precursor influenced the opaque and aggregated films as result of the presence of intermolecular hydrogen bonds between N–H and C=O on the acridone groups whereas N-methylated precursor functionalized PMO films were transparent, suggesting that capping of the amine group hindered the intermolecular hydrogen bonds and effectively suppressed aggregate formation during PMO films casting.[228] Kasja et al.[232] have reported that ligands with different p-conjugation lengths and side chains show impact on the optical properties. Direct modification of the ligands by using hydrophobic alkyl chains has been proven to effectively stabilize the particles. Different metal ions, donors, and acceptors have been incorporated into the frameworks by one-step coordination-directed assembly. Experimental results clearly show that the optical properties of nanoscale light-harvesting metal–organic frameworks (NMOFs) can be enhanced and tuned by chemical manipulation of the inorganic and organic components in the frameworks. The development of photocatalytic systems linked with light-harvesting function is also important.[234-240] Hirai et al.[237] have immobilized CdS nanoparticles into PMOs to be used as photocatalyst for the generation of H_2 from 2-propanol aqueous solution. It was shown that morphology, stability, and framework hydrophobicity have affected photocatalytic activity. On the other hand, Ti-functionalized PMO (Ti-PMO) was also found to be employed as a photocatalyst for selective olefin epoxidation.[210] The reaction rate on the Ti-containing PMO catalysts is similar to that on Ti-containing pure silica due to the destabilization of these oxygen radicals on the hydrophobic surface of the Ti-PMO catalysts. It is well-known that the O_3^- radical is a crucial oxidant for epoxide formation which is more destabilized once O_3^-radical is on the hydrophobic Ti-PMO surface. On the other hand, the hydrophobic olefins also easily access the photoexcited Ti-O_4 species on the hydrophobic Ti-PMOs surface. What happened then is that the destabilizations of the photoexcited Ti-O_4 species and O_3^- radical counteract the enhanced access of olefins to the excited species, resulting in almost no improvement in the olefin conversion.[238] In 2014, a visible-light harvesting antenna based on acridone groups functionalized PMO (Acd-PMO) was successfully synthesised using [RuII(bpy)$_3^{2+}$] complex (bpy=2,2/-bipyridyl) coupled with iridium oxide (IrOx) particles supported in the PMO meso channels framework as photosensitizer and catalyst, respectively.[239] It was found that Acd-PMO absorbed visible light and funnelled the light energy into the Ru complex on the meso channels through excitation energy transfer. From this study, the reaction quantum yield was 0.34 %, which was improved to 0.68% by the modifications of PMO.[239] Inagaki and co-workers[239] also reported surfactant-mediated PMO for an artificial photosynthesis system with three-dimensional organization of molecular parts, such as a light absorber and a Re-complex as the multi-electron catalyst. A rhenium (Re) bipyridine complex was chosen as a reaction centre as is a well-known two-electron-reduction photocatalyst for conversion of CO_2 to CO. This is a very new conceptual design for enhancing the photocatalytic CO_2 reduction of rhenium (I) complex placed in the mesochannels of PMO framework.

Another important study[241] has shown that biphenyl-bridged PMO was chosen due to its well-defined mesoporous framework and strong light absorption capacity where viologen functions and Pt were used as the electron acceptor and catalyst, respectively. The purpose of covalently attachment of viologen functions into the PMO framework is not only to create charge transfer (CT) complexes with the biphenyl segments but also to induce electron transfer from biphenyl segments to viologen to promote persistent charge separation.[241] It is also reported formation of a 100% benzene-bridged PMO bearing arenetricarbonyl complexes to produce a CT band from Cr to the benzene ring but no photocatalysis was occurred.[162] Therefore, Inagaki et al.[241] have employed Pt as a catalyst for H_2 evolution using Pt/Vio–Bp–PMO in the presence of reduced nicotinamide adenine dinucleotide (NADH) as a sacrificial agent (irradiation at 400 nm). A presumed mechanism was proposed in Fig. 25 for the charge separation.[241] In order to confirm this result, the use of homogeneous solution of Bp molecules, methylviologen, and colloidal Pt did not produce any H_2, due to a weaker electron-donating feature of molecular Bp than that of densely packed Bp in Bp–PMO. These results clearly indicated the importance of densely packed Bp and Vio within mesoporous structure for hydrogen evolution. Recently, visible-light absorbers acridone (Acd) and methyllacridone (MeAcd) were embedded in the pore walls of PMO to produce well-defined hybrid Acd-PMOs and MeAcd-PMOs.[242] The pore sizes of 4.6 and 3.7 nm for Acd–PMO and MeAcd–PMO, respectively, are providing enough space for encapsulation of Ru^{II}-Re^{I} complex which has van der Waals radii (ca. 2.4 nm). The encapsulation of Ru^{II} and Re^{I} in the PMOs

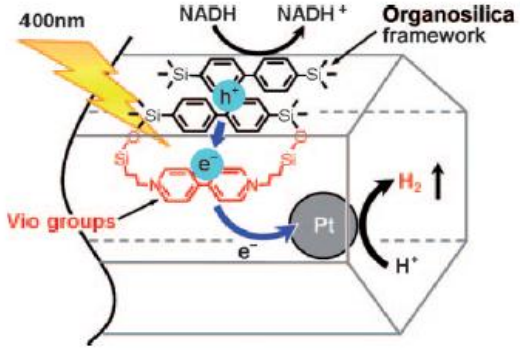

Fig. 25. Designed solid-state donor–acceptor system based on PMO for photocatalytic H_2 evolution. Photo-irradiation induces electron transfer from Bp in the framework to Viologen covalently attached to the framework. Pt in the mesochannels promotes H_2 evolution. Holes in the framework are consumed by oxidation of the sacrificial agent, Reproduced from ref 241 with permission from Wiley.

(Acd–PMO or MeAcd–PMO) was worked as photosensitizer and catalyst, respectively for CO_2 reduction.[242]

3.11 Hole-transporting function, optical and solar cell properties

As discussed previously, PMOs with different types of active organic bridging groups (R) ranging from aliphatic and aromatic hydrocarbons to heterocyclics and metal complexes could be used for various target oriented applications. Meanwhile, a number of PMOs with various organic groups including ethane, aromatic and Π-conjugated bridging groups have been reported with useful properties such as optical, strong light absorption, fluorescence, light harvesting and excitation energy transfer.[20-90,243-248] Recent aromatic organosilica materials have been reported with hole-transporting and optical functions.[59] It is anticipated that the emission and charge transport properties of the active organic material could be greatly affected by their confinement within the nanochannels of porous framework which may be well-suited for organic electronic applications such as light-emitting diodes, solar cells, and thin film transistors. Wahab et al.[59] have reported the use of evaporation induced self-assembly method (EISA) to organize and chemically bind a photoluminesent/hole transporting material. N,N/-bis(4-tert-butylphenyl)-N,N/-bis(4-((E)-2-(triethoxysilyl)vinyl)phenyl)biphenyl-4,4/-diamine (TEVS-TPD) was incorporated into the ordered nanochannels within an organosilica matrix based on 1,2-bis(triethoxysilyl)ethane (BTSE). This strategy was used to fabricate photoluminescent (PL) and charge transport (CT) groups functionalized nanocomposite thin films in-situ wherein the PL/CT material is confined and chemically bonded inside the nanochannels of the PMO. The resultant thin films show interesting photoluminescent and increased hardness properties over their non-ordered counterparts to strongly suggest that the pore channels are occupied by the functionalized material of interest. Later, TEVS-TPD has been used for evaluating the device performance as an improved alternative to Poly(3,4-ethylenedioxythiophene):poly(styrenesulfonate) PEDOT:PSS as application in organic light emitting diodes (OLEDs) and organic photovoltaics (OPVs) (Fig. 26).[243] The devices with cross-linked TEVS-TPD HITL (hole injection/transport layers) (10 nm thickness) exhibited lower turn-on voltage with lower leakage current, higher luminance and stability at high current density, and similar maximum efficiencies at low voltages as compared to those based on PEDOT:PSS HITL. In addition, the devices based on cross-linked TEVS-TPD exhibited device performances superior to those of the devices prepared with TEVS-TPD monomer or TEPCS-TPD polymer that contains insulating moieties between the silicon atom and the aromatic amine. Inagaki et al.[248] have reported the synthesis of a hole transporting periodic mesostructured organosilica (Fig. 27). The hole-transporting behavior of the mesostructured film was examined by TOF measurements. The hole mobility in mesostructured film was ~ 3.2 X 10-5 cm^2 V^{-1} s^{-1} that is slightly lower than that of the hole mobility (~5.1 × 10-5 cm^2 V^{-1} s^{-1}) determined by non-structured organosilica film. This study suggested that molecular packing of uncondensed precursor

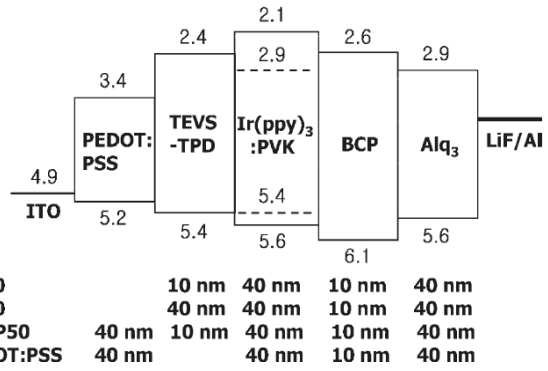

Fig. 26. Device structures [ITO/HITL (OS10,OS40, OSPP50, PEDOT: PSS)/Ir(ppy)3:PVKemissive layer (40 nm)/BCP (10 nm)/Alq3 (40 nm)/LiF (1 nm)/Al (100 nm)] and the corresponding energy level diagram. The energy levels of the materials except cross-linked TEVS-TPD are literature values, Reproduced from Ref 243 with permission from ACS Publications.

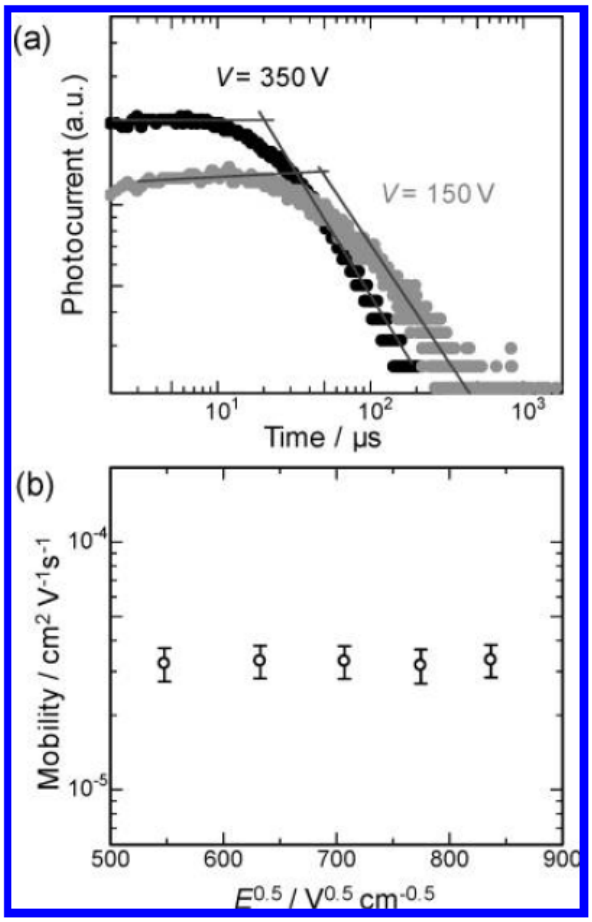

Fig. 27. (a) Double logarithmic plots of transient photocurrent of 1-Brij76-F (thickness: 5 μm) as a function of time at applied voltages of 150 and 350 V. (b) Plot of the hole mobility of 1-Brij76-F versus electric field strength, Reproduced from Ref 248 with permission from ACS Publications.

the crystal lattice may also impede hole hopping between organic moieties.

3.12 PMOs with electroactive functions and fuel cell application

The incorporation of electro active functions into the frameworks of PMOs has really shown much interest in developing redox catalysts, electrochemical sensor, electroluminescent systems and electronic devices.[20-26] For example, ethane-PMOs with arene-sulfonic acid groups have displayed an acid capacity and proton conductivity of 1.38 meq/g and 1.6 × 10−2 S/cm respectively.[249] PMOs functionalized with electroactive bridged silsesquioxane precursor, N,N'-bis(4'-(3-triethoxysilylpropylureido) phenyl)-1,4-quinonene-diimine (TSUPQD) has shown similar electrochemical behavior as polyaniline but with slightly higher redox peak potentials which are attributed to the electron withdrawing ureidopropyl groups attached to the main chain of the amino-capped aniline trimer.[250] One well defined redox pair of peaks was found at around 0.55 V against the reference electrode (Ag/AgCl) which corresponds to the transition from the "leucoemeraldine" to the "emeraldine" form of the aniline oligomer and represents the removal/addition of two electrons. The second redox pair of peaks which corresponds to the oxidation of the "emeraldine" form to the "pernigraniline" form cannot be detected in aqueous solution due to the background range limit from water. In addition, the conductivity measurement was conducted (10.5 Scm^{-1}) for HCl-doped 66 wt% TSU-PMO using a four-probe method. In contrast to the aniline trimer, this measurement shows a two orders of magnitude decrease in conductivity, which arises from the presence of the non-conducting inorganic silica framework.

3.13 Low dielectric layers for microelectronics application

An ultra-low-k layer semiconductor is a material with a dielectric constant (k) much smaller than that of the silicon dioxide used in chips (aprox. 4). The development of novel synthetic strategies is necessary for advancing technologies in the semiconductor industry. Ultralow *k* layers (*k* < 2.0) are required for designing modern ICs and other digital devices. It is found to be difficult to make such devices with compact and dense materials with low-*k* less than 2. In this context, PMOs can play important role because of high amount of hydrophobic organic segments in the framework, which could easily be polarised only to a lesser extent than SiO_2.[251-258] Ozin et al.[252] have reported spin-coated 1,3,5-tris[diethoxysila]cyclohexane $[(EtO)_2SiCH_2]_3$ cyclic silsesquioxane based PMO thin films with low *k* values about 2. Interestingly, the dielectric *k* values of PMO thin films are found to decrease linearly with increasing loading of organic functional groups. Same group has reported PMO thin film of octavinyl polyhedral oligomeric silsesquioxane (OVPOSS)(octa(triethoxysilylethyl)POSS ($POSS[C_2H_4Si(OEt)_3]_8$).[255] The final PMO film has decreased dielectric constant (*k*) from 2.03 (pure POSS film) to 1.73 (OV-POSS-PMO film) due to the 10-fold increase in the porosity of the POSS-PMO. Recently, Driesscche et al.[258] have reported a new procedure to seal the pores of mesoporous low-*k* films

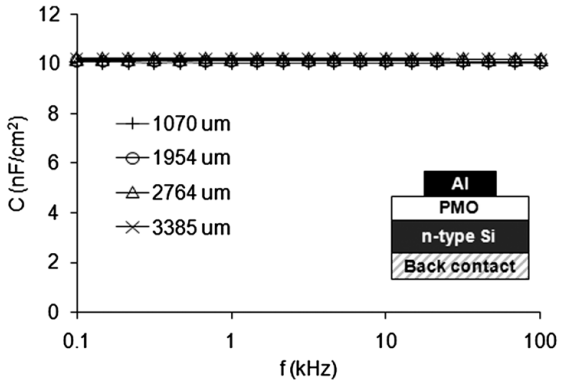

Fig. 28. Measured accumulation capacitance per unit area as a function of frequency for the four dots of different diameters, Reproduced from Ref. 258 with permission from the Royal Society of Chemistry.

using a pre-condensed organosilica oligomers pore sealing method for the preparation of low-*k* mesoporous ethylene-bridged organosilica films.[257] The *k*-value of the non-sealed ethylene-bridged organosilica film was 2.15 for a porosity of 39.5% whereas after the sealing the porosity decreases to 38% and the *k*-value only slightly increases to 2.22. Even more, no water adsorption was observed on the sealed films. These results show that the sealing almost has no impact on the overall *k*-value and thus a huge step forward is achieved in sealing mesoporous low-*k* materials. In addition, ultra-low-*k* cyclic carbon-bridged PMO films have not only a high chemical resistance but also are hydrophobic and crack-free highly porous films with low-*k* value of 1.8.[258] Fig. 28 suggested that the dielectric constant is stable with frequency as it is expected for hydrophobic low-*k* films in the explored frequency range.[2-] The main text of the article should appear here with headings as appropriate.

Conclusions

This review has clearly demonstrated the recent advances of PMOs with various organic functionalities in the framework for functional group based applications since they were firstly synthesized in 1999. It is found that the intelligent design and synthesis of PMO structures along with new functional groups can provide a completely new application portfolio. For example, studies of PMOs with novel organic functional groups such as chromophores, fluorophores, light-harvesting group, electroactive species and metal complexes have clearly shown advances in the fields of luminescence, opto-electronic devices, solid-state catalysts, and solid state photoreaction systems. For clearer example, a photocatalytic system for CO_2 reduction exhibiting visible light harvesting was developed by preparing a hybrid consisting of a supramolecular metal complex as photocatalyst and PMO as light harvester, indicating the influence of chemical structure of organic functional groups in the framework. Moreover, the use of PMOs in biomedical science could be considered as a remarkable advance. Very recently, an efficient and versatile chemical homology principle

to synthesize a new family of third-generation PMO nanoparticles with multiple organic groups incorporated within the organosilica framework known as hybridized hollow PMO nanoparticles has been reported for biomedicine.[157] In particular, the integration of physiologically active thioethergroups with disulfide bonds has enabled unique reducing and HIFU-responsive drug-releasing performance, specific biological effects, and enhanced ultrasonography behavior for HMONs-based drug delivery systems. Importantly, the Dox loaded PMO nanoparticles exhibited enhanced antitumor therapeutic efficiency both *in-vitro* and *in-vivo*. The MPMO NPs (known as mixed PMO nanoparticles) were found to be very efficient for anti-cancer drug delivery combined with two-photon therapy in MCF-7 breast cancer cells, leading down to 76% cancer cell death. MPMO NPs are thus very promising for nanomedicine applications. These PMOs provide great possibilities for designing suitable host-matrices for targeted application through the careful design of suitable bridges that are able to interact with functional groups of the tested drugs. These studies on PMOs suggest the control ability of the drug loading and their subsequent release. The good biocompatibility and low cytotoxicity of PMOs open challenging opportunities for the use of PMOs as biomaterials in the future. However, some aspects related to pore orientation for biomedical and other devices have to be carefully studied and remain still a research challenge. For example, PMOs with perpendicular pore channels to surface/any substrate have not been studied since electron transfer and motion of biological molecules related to electron transfer are found to depend on the pore orientation. More importantly when any molecules are confined by pore can significantly impact on the final properties including kinetics and releasing profile and so many other properties.

In another field, PMOs synthesized with different morphologies can be directly converted into unique porous carbon structures (pore channels could be changed) depending on the starting reacting materials/precursors. This approach could be extended as a general strategy to prepare ordered mesoporous carbon structures with diverse compositions and morphologies simply by replacing silica from the framework. Similarly, PMOs with nitrogen functions under desired conditions can be converted into carbon nitride and related materials.

Acknowledgements

Authors acknowledge the support received for this manuscript from Nanomaterials Centre of Australian Institute for Bioengineering and Nanotechnology, The University of Queensland, Australia.

List of acronyms used in this paper

Full Name	Code
1,2-bis(triethoxysilyl)ethane	BTSE
3-aminopropyltrimethoxysilane	3-APTMOS
2,9-Dimethyl-4,7-diphenyl-1,10-phenanthroline	BCP
Arene sulfonic acid ethane-silica	AS-MES
Arenetricarbonyl complexes	[PhM(CO)3] (M = Cr, Mo)
Acridone functionalized PMO	Acd-PMO
Bis-(triethoxysilyl)ethylene	BTEEE
Bis(triethoxysilyl)phenylene	BTEB
Bis-(triethoxysilyl)ethane	BTEE
Bis(triethoxysilyl)-biphenyl	BTEBP
Bis-triethoxysilyl-binapthyl	BINAP
Charge transport	CT
Confocal laser scanning microscopy	CLSM
Doxorubicin	Dox
$(EtO)_3Si–R–Si(OEt)_3$	R for ethane, methane, benzene, biphenyl, whereas Eto is for ethoxy group
Ethane-bis(propyl)ethylenediamine silica	EBPEDS
Evaporation-induced self-assembly	EISA
Glutathione	GSH
High performance liquid chromatography	HPLC
Hole injection/transport layers	HITL
Hollow morphology of PMO	HPMO

Horseradish peroxidase	HRP
Light-harvesting metal–organic frameworks	NMOF
Magnetic resonance imaging	MRI
Mobil Composition of Matter	MCM
N,N/-disilylated pyridine-bridged periodic mesoporous organosilicas	DMPy-PMOs
N,N'-bis(4'-(3-triethoxysilylpropylureido) phenyl)-1,4-quinonene-diimine	TSUPQD
N,N/-bis[3-(trimethoxysilyl)propyl]-ethylenediamine	BTSPED
N,N/-bis(4-tert-butylphenyl)-N,N/-bis(4-((E)-2-(triethoxysilyl)vinyl)phenyl)bipheny l-4,4/-diamine	TEVS-TPD
Organic light emitting diodes	OLEDs
Organic photovoltaic	OPV
Pentyl-linked bis(rhodamine)-	PRh
Periodic mesoporous organosilica	PMO
Phosphate buffer solution	PBS
Photoluminescent	PL
Poly(3,4-ethylenedioxythiophene):poly(styr enesulfonate)	PEDOT:PSS
Poly(3,4-ethylenedioxythiophene	PEDOT
Poly(styrenesulfonate)	PSS
Pure mesoporous silica	PMS
Reversed phase liquid chromatography	RPLC
Rhenium	Re
Simulated body fluid	SBF
Tetracycline	TC
Tetraethyl orthosilicate	TEOS
Tris(8-hydroxyquinolinato)aluminum	Alq3

Notes and references

1 J. S. Beck, J. C. Vartuli, W. J. Roth, M. E. Leonowicz, C. T. Kresge, K. D. Schmitt, C. T. W. Chu, D. H. lson, E. W. Sheppard, S. B. McCullen, J. B. Higgins and J. L. Schlenker, *J. Am. Chem. Soc*., 1992, **114**, 10834-10843.

2 A. Kuperman, S. Nadimi, S. Oliver, G. A. Ozin, J. M. Garces and M. M. Olken, *Nature*, 1993, **365**, 239-242.

3 S. Inagaki, Y. Fukushima and K. Kuroda, *J. Chem. Soc. Chem. Commun*., 1993, 680-683.

4 S. L. Burkett, S. D. Sims and S. Mann, *Chem. Commun*., 1996, 1367-1368.

5 D. J. Macquarrie, *Chem. Commun*., 1996, 1961-1962.

6 G. Cerveau, R. J. P. Corriu, E. Framery and F. Lerouge, *Chem. Mater*. 2004, **16**, 3794-3799.

7 D. A. Loy, G. M. Jamison, B. M. Baugher, S. A. Myers, R. Assink and K. J. Shea, *Chem. Mater*. 1996, **8**, 656-663.

8 B. Boury, R. J. P. Corriu and Vale´rie Le Strat, *Chem. Mater*. 1999, **11***,* 2796-2803.

9 D. A. Loy and Kenneth J. Shea, *Chem. Rev*. 1995, **95**, 1431-1442.

10 G. Cerveau, S. Chappellet, R. J. P. Corriu, B. Dabiens and J. L. Bideau, *Organometallics,* 2002**, 21***,* 1560-1564.

11 D. A. Loy, B. M. Baugher, C. R. Baugher, D. A. Schneider and K. Rahimian, *Chem. Mater*. 2000, **12**, 3624-3632.

12 H. Skar, J. G. Seland, Y. Liang, N. A. Frøystein, K. W. Törnroos and R. Anwander, *Eur. J. Inorg. Chem*. 2013, 5969–5979.

13 V. Morales, J. A. Villajos, R. A. Garcıa, J. Mater. Sci., 2013, **48**, 5990–6000.

14 Y. Liang and R. Anwander, *Dalton Trans*., 2013, **42**, 12521–12545.

15 A. Corma, *Chem. Rev*., 1997, **97**, 2373-2420.

16 D. Y. Zhao, J. L. Feng, Q. S. Huo, N. Melosh, G. H. Fredrickson, B. F. Chmelka and G. D. Stucky, *Science*, 1998, **279**, 548–552.

17 M. H. Lim, C. F. Blanford and A. Stein, *J. Am. Chem. Soc*., 1997, **119**, 4090-4091.

18 C. H. Zhou, X. Xia, C. X. Lin, D. S. Tonga and J. N. Beltramini, *Chem. Soc. Rev*., 2011, **40**, 5588–5617.

19 J. Y. Ying, C. P. Mehner and M. S. Wong, *Angew. Chem. Int. Edn*., 1999, **38**, 56-77.

20 B. Hatton, K. Landskron, W. Whitnall, D. Perovic and G. A. Ozin, *Acc. Chem. Res*. 2005, **38**, 305–312.

21 S. S. Park, M. S. Moorthy and C. S. Ha. *NPG Asia Materials*, 2014, **6**, e96; doi:10.1038/am.2014.13.

22 N. Mizoshita, T. Taniab and S. Inagaki, *Chem. Soc. Rev*., 2011, **40**, 789–800.

23 C. H. Zhou, J. N. Beltramini, Y. X. Fan and Max. Lu, *Chem. Soc. Rev*., 2008, **37**, 527–549

24 F. Hoffmann, M. Cornelius, J. Morell and M. Froba, *Angew. Chem. Int. Edn*., 2006, **45**, 3216–3251.

25 M. Jaroniec, *Nature*, 2006, **442**, 638–640.

26 W. Wang, J. E. Lofgreen and G. A. Ozin, *Small*, 2010, **6**, 2634–2642.

27 P. V. D. Voort, D. Esquivel, E. D. Canck, F. Goethals, I. V. Driessche and F. J. Romero-Salguero, *Chem. Soc. Rev*., 2013, **42**, 3913–3955.

28 F. Hoffmann and M. Froba, *Chem. Soc. Rev*., 2011, **40**, 608–620.

29 S. Inagaki, S. Guan, T. Ohsuna and O. Terasaki, *Nature*, 2002, **416**, 304-307.

30 M. P. Kapoor and S. Inagaki, *Bull. Chem. Soc. Jpn*., 2006, **79**, 1463–1475.

31 W. J. Hunks and G. A. Ozin, *J. Mater. Chem*., 2005, **15**, 3716-3724.

32 A. Stein, B. J. Melde and R. C. Schroden, *Adv. Mater.*, 2000, **12**, 1403-1419.

33 A. Sayari and S. Hamoudi, *Chem. Mater.*, 2001, **13**, 3151-3168.

34 A. Sayari and P. Liu, *Micropor. Mesopor. Mater*., 1997, **12**, 149-177.

35 A. Bhaumik and T. Tatsumi, *J. Catal.*, 2000, **189**, 31-39.

36 F. Babonneau, L. Leite and S. Fontlupt, *J. Mater. Chem.*, 1999, **9**, 175-178.

37 A. Corma, J. L. Jorda, M. T. Navarro and F. Rey, *Chem. Commun*., 1998, 1899-1900.

38 W. M. V. Rhijin, D. E. D. Vos, B. F. Sels, W. D. Bossaert and P. A. Jacobs, *Chem. Commun*., 1998, 317-318.

39 J. Liu, Y. Shin, Z. Nie, J. H. Chang, L. Q. Wang, G. E.Fryxell, W. D. Samuels and G. J. Exarhos, *J. Phys. Chem. A*, 2000, **104**, 8328-8339.

40 S. Inagaki, S. Guan, Y. Fukushima, T. Ohsuna and O. Terasaki, *J. Am. Chem. Soc*., 1999, **121**, 9611-9614.

41 B. J. Melde, B. T. Holland, C. F. Blanford and A. Stein, *Chem. Mater*., 1999, **11**, 3302-3308.

42 T. Asefa, M. J. MacLachlan, N. Coombs and G. A. Ozin, *Nature*, 1999, **402**, 867-871.

43 C. Yoshina-Ishii, T. Asefa, N. Coombs, M. J. MacLachlan and G. A. Ozin, *Chem. Commun*., 1999, 2539-2540.

44 S. Guan, S. Inagaki, T. Ohsuna and O. Terasaki, *J. Am. Chem. Soc*., 2000, **122**, 5660-5661.

45 A. Sayari, S. Hamoudi, Y. Yang, I. L. Moudrakovski and J. R. Ripmeester, *Chem. Mater*., 2000, **12**, 3857-3863.

46 D. Zhang, J. Xu, Q. Zhao, T. Cheng and G. Liu, *ChemCatChem,* 2014, **6**, 2998 – 3003.

47 M. P. Kapoor and S. Inagaki, *Chem. Mat*er., 2002, **14**, 3509-3514.

48 M. Kruk, M. Jaroniec, S. Guan and S. Inagaki, *J. Phys. Chem. B*, 2001, **105**, 681-689.

49 T. Asefa, M. J. MacLachlan, H. Grondey, N. Coombs and G. A. Ozin, *Angew. Chem. Int. Ed.*, 2000, **39**, 1808-1811.

50 S. Hamoudi, Y. Yang, I. L. Moudrskovski, S. Lang and A. Sayari, *J. Phys. Chem. B*, 2001, **105**, 9118-9123.

51 H. G. Zhu, D. J. Jones, J. Zajac, J. Roziere and R. Dutartre, *Chem. Commun*., 2001, 2568–2569.

52 H. I. Lee, C. Pak, S. H. Yi, J. K. Shon, S. S. Kim, B. G. So,H. Chang, J. E. Yie, Y. U. Kwon and J. M. Kim, *J. Mater. Chem*., 2005, **15**, 4711-4717.

53 M. A. Wahab, I. Kim and C. S. Ha, *J. Solid- State Chem.,* 2004, **177**, 3439–3447.

54 M. A. Wahab, H. Q. Eliza, X. H. Lu and C. B. He. *Soft Mater*., 2010, **8**, 183–196.

55 M. A. Wahab and C. B. He, *Soft Mater*., 2009, **7**, 79–92.

56 M. A. Wahab, H. Hussain and C. B. He, *Langmuir*, 2009, **25**, 4743-4750.

57 M. A. Wahab and C. B. He, *Langmuir*, 2009, **25**. 832-838.

58 M. A. Wahab and C. B. He, *J. Nanosci. Nanotechnol*., 2008, **8**, 6381-6386.

59 M. A. Wahab, S. Sudhakar, Y. Elaine and A. Sellinger, *Chem. Mater*., 2008, **20**, 1855-1861.

60 M. A. Wahab, I. Kim and C. S. Ha, *J. Nanosci. Nanotechnol*., 2008, **8**, 3532-3538.

61 M. A. Wahab and A. Sellinger, *Chem. Lett*., 2006, **35**, 1240-1241.

62 M. A. Wahab, I. Imae, Y. Kawakami and C. S. Ha, *Micropor. Mesopor. Mater*., 2006, **92**, 201-211.

63 M. A. Wahab, I. Imae, Y. Kawakami and C. S. Ha, *Chem. Mater*., 2005, **17**, 2165-2174.

64 M. A. Wahab and C. S. Ha, *J. Mater. Chem*., 2005, **15**, 508-516.

65 M. A. Wahab, I. Kim and C. S. Ha, *J. Solid-State. Chem*., 2004, **177**, 3439-3447.

66 M. A. Wahab, I. Kim and C. S. Ha, *Micropor. Mesopor. Mater*., 2004, **69**, 19-27.

67 M. A. Wahab, S. S. Chu, C. Anand and C. S. Ha, *J. Nanosci. Nanotechnol*., 2012, **12**, 4531–4539.

68 S. Hamoudi and S. Kaliaguine, *Chem. Commun*., 2002, 2118-2119.

69 O. Muth, C. Schellbach and M. Froba, *Chem. Commun*., 2001, 2032-2033.

70 M. C. Burleigh, M. A. Markowitz, M. S. Spector and P. B. Gaber, *J. Phys. Chem. B*, 2001, **105**, 9935-9942.

71 J. R. Matos, M. Kurk, L. P. Mercuri, M. Jeroniec, T. Asefa,N. Coombs, G. A. Ozin, T. Kamiyama and O. Terasaki, Chem. Mater., 2002, **14**, 1903-1905.

72 C. Yu, Y. Yu and D. Zhao, *Chem. Commun*., 2000, 575-576.

73 W. Guo, J. Y. Park, M. O. Oh, H. W. Jeong, W. J. Cho, I. Kim and C. S. Ha, *Chem. Mater.*, 2003, **15**, 2295-2298.

74 W. Guo, I. Kim and C. S. Ha, *Chem. Commun*., 2003, 2692-2693.

75 K. Nakajima, D. Lu, I. Tomita, S. Inagaki, M. Hara, S.Hayashi, K. Domen and J. N. Kondo, *Chem. Lett*., 2003, **32**, 950-951.

76 W. Wang, S. Xie, W. Zhou and A. Sayari, *Chem. Mater*., 2004, **16**, 1756-1762.

77 K. Nakajima, I. Tomita, M. Hara, S. Hayashi, K. Domen and J. N. Kondo, *J. Mater. Chem.*, 2005, **15**, 2362-2368.

78 M. P. Kapoor, N. Setoyama, Q. Yang, M. Ohashi and S. Inagaki, *Langmuir*, 2005, **21**, 443.

79 Y. Goto and S. Inagaki, *Chem. Commun*., 2002, 2410-2411.

80 G. Temtsin, T. Asefa, S. Bittner and G. A. Ozin, *J. Mater.Chem*., 2001, **11**, 3202-3206.

81 M. Kuroki, T. Asefa, W. Whitnal, M. Kruk, C. Yoshina-Ishii, M. Jaroniec and G. A. Ozin, *J. Am. Chem. Soc*., 2002, **124**, 13886-13895.

82 K. Landskron, B. D. Hatton, D. D. Perovic and G. A. Ozin, *Science*, 2003, **302**, 266-269.

83 K. Landskron and G. A. Ozin, *Science*, 2004, **306**, 1529-1532.

84 W. J. Hunks and G. A. Ozin, *Chem. Commun*., 2004, 2426-2427.

85 W. J. Hunks and G. A. Ozin, *Chem. Mater*., 2004, **16**, 5465-5472.

86 J. Morell, G. Wolter and M. Froba, *Chem. Mater*., 2005, **17**, 804-808.

87 K. Okamoto, Y. Goto and S. Inagaki, *J. Mater. Chem*., 2005, **15**, 4136-4140.

88 N. Bion, P. Ferreira, A. Valente, I. S. Goncalves and J. Rocha, *J. Mater. Chem*., 2003, **13**, 1910-1913.

89 B. Onida, L. Borello, C. Busco, P. Ugliengo, Y. Goto, S. Inagaki and E. Garrone, *J. Phys. Chem*., 2005, **109**, 11961-11966.

90 Y. Goto, K. Okamoto and S. Inagaki, *Bull. Chem. Soc. Jpn*., 2005, **78**, 932-936.

91 M. P. Kapoor, Q. Yang and S. Inagaki, *Chem. Mater*., 2004, **16**, 1209-1213.

92 M. P. Kapoor, Q. Yang and S. Inagaki, *J. Am. Chem. Soc*., 2002, **124**, 15176-15177.

93 T. Shimada, K. Aoki, Y. Shinoda, T. Nakamura, N.Tokunaga, S. Inagaki and T. Hayashi, *J. Am. Chem. Soc*., 2003, **125**,4688-4689.

94 M. P. Kapoor, S. Inagaki, S. Ikeda, K. Kakiuchi, M. Suda and T. Shimada, *J. Am. Chem. Soc*., 2005, **127**, 8174-8178.

95 K. Kamoto, M. P. Kapoor and S. Inagaki, *Chem. Commun*., 2005, 1423-1424.

96 Y. Xia, W. Wang and R. Mokaya, *J. Am. Chem. Soc*., 2005,**127**, 790-798.

97 W. Wang, W. Zhou and A. Sayari, *Chem. Mater*., 2003, **15**, 4886-4889.

98 A. Sayari and W. Wang, *J. Am. Chem. Soc*., 2005, **127**, 12194-12195.

99 J. Liu, H. Q. Yang, F. Kleitz, Z. G. Chen, T. Yang, E. Strounina, Max Lu and S. Z. Qiao, *Adv. Funct. Mater*., 2012, **22**, 591-599.

100 S. Z. Qiao, C. X. Lin, Y.G. Jin, Z. Li, Z. Yan, Z. P. Hao, Y.N. Huang and Max. Lu. *J. Phys. Chem. C,* 2009, **113**, 8673-8682.

101 C. X. Lin, S. Z. Qiao, C. Z. Yu, S. Ismadji and Max Lu, *Micropor. Mesopor. Mater*., 2009, **117**, 213-219.

102 L. Zhang, S. Z. Qiao, Y.G. Jin, Z.G. Chen, H. C. Gu and M. Lu, *Adv. Mater*., 2008, **20**, 805-809.

103 J. Brown, L. Mercier and T. J. Pinnavaia, *Chem. Commun*., 1999, 69-70.

104 T. Asefa, M. Kruk, M. J. MacLachlan, N. Coombs, H.Grondey, M. Jaroniec and G. A. Ozin, *J. Am. Chem. Soc*., 2001, **1235**, 8520-8530.

105 X. Wu, S. Ji, Y. Li, B. Li, X. Zhu, K. Hanabusa and Y. Yang, *J. Am. Chem. Soc*., 2009, **131**, 5986–5993.

106 S. MacQuarrie, M. P. Thompson, A. Blanc, N. J. Mosey, R. P. Lemieux and C. M. Crudden, *J. Am. Chem. Soc*., 2008, **130**, 14099–14101 .

107 X. Wu and C. M. Crudden, *Chem. Mater*., 2012, **24**, 3839−3846.

108 G. Zhu, H. Zhong, Q. Yang and C. Li, *Micropor. Mesopor. Mater*., 2008, **116**, 36–43.

109 T. Seki, K. McEleney and C. M. Crudden, *Chem. Commun*., 2012, **48**, 6369–6371.

110 A. Kuschel and S. Polarz, *J. Am. Chem. Soc*., 2010, **132**, 6558–6565.

111 J. Morell, S. Chatterjee, P. J. Klar, D. Mauder, I. Shenderovich, H. Hoffmann and M. Froba, *Chem. Eur. J*., 2008, **14**, 5935–5940.

112 X. Wu, S. Ji, Y. Li, B. Li, X. Zhu, K. Hanabusa and Y. Yang, *J. Am. Chem. Soc*., 2009, **131**, 5986–5993.

113 S. MacQuarrie, M. P. Thompson, A. Blanc, N. J. Mosey, R. P. Lemieux and C. M. Crudden, *J. Am. Chem. Soc*., 2008, **130**, 14099–14101 .

114 X. Wu and C. M. Crudden, *Chem. Mater*., 2012, **24**, 3839−3846.

115 G. Zhu, H. Zhong, Q. Yang and C. Li, *Micropor. Mesopor. Mater*., 2008, **116**, 36–43.

116 T. Seki, K. McEleney and C. M. Crudden, *Chem. Commun*., 2012, **48**, 6369–6371.

117 A. Kuschel and S. Polarz, *J. Am. Chem. Soc*., 2010, **132**, 6558–6565.

118 J. Morell, S. Chatterjee, P. J. Klar, D. Mauder, I. Shenderovich, H. Hoffmann and M. Froba, *Chem. Eur. J*., 2008, **14**, 5935–5940.

119 Y. Li, S. Wang, M. Xiao, M. Wang, Z. Huang, B. Li and Y. Yang, *Nanotechnology*, 2013, **24**, 035603-8.

120 X. Meng, T. Yokoi, D. Lu and T. Tatsumi, *Angew. Chem. Int. Ed.*, 2007, **46**, 7796 –7798.

121 B. Li, Z. Xu, W. Zhuang, Y. Chen, S. Wang, Y. Li, M. Wang and Y. Yang, *Chem. Commun*., 2011, **47**, 11495–11497.

122 V. Jayalakshmi, T. Wood, R. Basu, J. Du, T. Blackburn, C. Rosenblatt, C. M. Crudden and R. P. Lemieux, *J. Mater. Chem*., 2012, **22**, 15255–15261.

123 T. T. Hao, J. Y. Shi, T. Y. Zhuang, W. D. Wang, F. C. Lia and W. Wang, *RSC Advances*, 2012, **2,** 2010–2014.

124 M. W. A. MacLean, T. K. Wood, G. Wu, R. P. Lemieux and C. M. Crudden, *Chem. Mater*. 2014, **26**, 5852−5859.

125 J. J. E. Moreau, L. Vellutini, M. W. Chi Man and C. Bied, *J. Am. Chem. Soc*., 2001, **123**, 1509-1510.

126 R. A. García-Munnoz, V. Morales, M. Linares and B. Rico-Oller, *Langmuir*, 2014, *30*, 881−890.

127 J. J. E. Moreau, L.Vellutini, M. W. Chi Man and C. Bied, *Chem. Eur. J*., 2003, **9**, 1594-1599.

128 S. Polarz and A. Kuschel, *Adv. Mater*. 2006, **18**, 1206–1209.

129 M. W. A. MacLean, L. M. Reid, X. Wu and C. M. Crudden, *Chem. An Asian J.,* 2015, **10,** 70-82**.**

130 Y. Jiang, X. Liu, Y. Chen, L. Zhou, Y. He, L. Ma and J. Gao, *Bioresour. Technol.*, 2014, **153**, 278–283.

131 B. Karimi,, H. M. Mirzaei and A. Mobaraki, *Catal. Sci. Technol*., 2012, **2**, 828–834

132 Z. Zhou, R. N. K. Taylor, S. Kullmann , H. Bao and M. Hartmann, *Adv. Mater*., 2011, **23**, 2627–2632.

133 S. E. Diez, E. I. Diaz and R. M. A. Blanco, *Micropor. Mesopor. Mater*., 2010, **132**, 487–493.

134 N. Li, J. G. Wang, H. J. Zhou, P. C. Sun and T. H. Chen, *Chem. Mater*., 2011, **23**, 4241–4249.

135 W. Na, Q. Wei, J. N. Lan, Z. R. Nie, H. Sun and Q. Y. Li, *Micropor. Mesopor. Mater*., 2010, **134**, 72–78.

136 S. Shylesh, A. Wagener, A. Seifert, S. Ernst and W. R. Thiel, *Angew. Chem. Intl. Edn*., 2010, **49**, 184-187.

137 C. M. Jimenez, J. Croissant, M. Maynadier, X. Cattoen, M. W. C. Man, J. Vergnaud, V. Chaleix, V. Sol, M. Garcia, M. Gary-Bobo, L. Raehma and J. O. Durand, *J. Mater. Chem. B,* 2015, **3**, 3681-3684.

138 M. Beretta, J. Morell, P. Sozzani and M. Froba, *Chem. Commun*., 2010, **46**, 2495–2497.

139 M. Bhattacharyya, P. Hiwale, M. Piras, L. Medda, D. Steri, M. Piludu, A. Salis and M. Monduzzi, *J. Phys. Chem. C*, 2010, **114**, 19928–19934.

140 J. Croissant, D. Salles, M. Maynadier, O. Mongin, V. Hugue[illegible] M. B. Desce, X. Cattoën, M. W. C. Man, A. Gallud, M. Garci[illegible],

M. G. Bobo, L. Raehm and J. O. Durand, *Chem. Mater.,* 2014, **26**, 7214−7220.

141 Z. Zhou, A Inayat, W. Schwieger and M Hartmann. *Micropor. Mesopor. Mater*., 2012, **154**, 133–141.

142 J. Gan, Z. Zhu, G Yan, Y Liu, P. Yang and B. Liu, *Anal. Chem*., 2012, **84**, 5809–5815.

143 K. Qian, W. Gu, P Yuan, F Liu, Y. Wang, M. Monteiro and C. Yu, *Small*, 2012, **8**, 231–236.

144 Y. Zhou, M. M. Wan, L Gao, N Lin, W. G. Lin and J. H. Zhu, *J. Mater. Chem. B*, 2013, **1**, 1738–1748.

145 B. Nohair, P. T. H. Thao, V. T. H. Nguyen, P. Q. Tien, D. T. Phuong, L. G. Hy and S. Kaliaguine, S. *J. Phys. Chem. C*, 2012, **116**, 10904–10912.

146 Na. Wei, W. Qi and Z. Nieuoren, *J. Mater. Chem*., 2012, **22**, 9970–9974.

147 C. X. Lin, Z. Li, S. Brumbley, L. Petrasovits, R. McQualter, C. Yu and Max Lu, *J. Mater. Chem*., 2011, **21**, 7565–7571.

148 M. Park, S. S. Park, S. Selvaraj, I. Kim and C.S. Ha, *J. Porous Mater*., 2011, **18**, 217–223.

149 M. S. Moorthy, M. J. Kim, J. H. Bae, S. S. Park, N. Saravanan, S. H. Kim and C. S. Ha. *Eur. J. Inorg. Chem*., 2013, 3028–3038.

150 C. X. Lin, S. Z. Qiao, C. Z. Yu, S. Ismadji and Max Lu, *Micropor. Mesopor. Mater*., 2009, **117**, 213–219.

151 M. Rat, M. H. Zahedi-Niaki, S. Kaliaguine and T. O. Do, *Micropor. Mesopor. Mater.*, 2008, **112**, 26–31.

152 C. Li, J. Liu, L. Zhang, J. Yang and Q. Yang, *Micropor. Mesopor. Mater*., 2008, **113**, 333–342.

153 F. X. Zhu, W. Wang and H. X. Li, *J. Am. Chem. Soc*., 2011, **133**, 11632–11640.

154 E. Y. Jeong, A. Burri, S. Y. Lee and S. E. Park, *J. Mater. Chem*., 2010, **20**, 10869–10875.

155 B. Karimi and F. K. Esfahani, *Chem. Commun*., 2011, **47**, 10452–10454.

156 B. Karimi, D. Elhamifar, J. H. Clark and A. J. Hunt, *Org. Biomol. Chem*., 2011, **9**, 7420-7426.

157 Y. Chen, Q. S. Meng, M. Wu, S. Wang, P. Xu, H. Chen, Y. Li, L. Zhang, L. Z. Wang and J. Shi, *J. Am. Chem. Soc*., 2014, **136**, 16326–16334.

158 D. Esquivel, E. D. Canck, C. J. Sanchidri, P. V. D. Voort and F. J. R. Salguero, *J. Mater. Chem*., 2011, **21**, 10990–10998

159 M. Ohashi, M. P. Kapoor and S. Inagaki, *Chem. Commun*., 2008, 841–843.

160 M. P. Kapoor, Y. Kasama, T. Yokoyama, M. Yanagi,S. Inagaki, N. Hironobu and L. R. Juneja, *J. Mater. Chem*., 2006, **16**, 4714–4722.

161 S. E. Hankari, B. Motos-Perez, P. Hesemann, A. Bouhaouss and J. J. E. Moreau, *J. Mater. Chem*., 2011, **21**, 6948–6955.

162 T. Kamegawa, T. Sakai, M. Matsuoka and M. Anpo, *J. Am. Chem. Soc*., 2005, **127**, 16784-16785.

163 C. Baleizao, B. Gigante, D. Das, M. Alvaro, H. Garcia and A. Corma, *J. Catal*., 2004, **223**, 106–113.

164 A. Corma, D. Das, H. Garcia and A. Leyva, *J. Catal*., 2005, **229**, 322–331.

165 F. Zhang, C. M. Kang, Y. Y. Wei and H. X. Li, *Adv. Funct. Mater*., 2011, **21**, 3189–3197.

166 J. L. Huang, F. X. Zhu, W. H. He, F. Zhang, W. Wang and H. X. Li, *J. Am. Chem. Soc*., 2010, **132**, 1492–1493.

167 C. M. Kang, J. L. Huang, W. H. He and F. Zhang, *J. Organomet. Chem.*, 2010, **695**, 120–127.

168 E. Y. Jeong, M. B. Ansari and S. E. Park, *ACS Catal*., 2011, **1**, 855–863.

169 V. Dufaud, F. Beauchesne and L. Bonneviot, *Angew. Chem. Int. Ed*., 2005, **44**, 3475–3477.

170 X. S. Yang, F. X. Zhu, J. L. Huang, F. Zhang and H. X. Li, *Chem. Mater*., 2009, **21**, 4925–4933.

171 Y. Yang, Y. Zhang, S. J. Hao and Q. B. Kan, *J. Colloid Interface Sci*., 2011, **362**, 157–163.

172 X. Wang, D. Lu, R. Austin, A. Agarwal, L. J. Mueller, Z. Liu, J. Wu and P. Feng, *Langmuir*, 2007, **23**, 5735-5739.

173 D. I. Fried, F. J. Brieler and M. Froba, *ChemCatChem*, 2013, **5**, 862 – 884.

174 J. Gan, J. Zhu, G. Yan, Y. Liu, P. Yang and B. Liu, *Anal. Chem*., 2012, **84**, 5809−5815.

175 Y. M. Huh, Y. W. Jun, H. T. Song, S. Kim, J. S. Choi, J. H. Lee, S. Yoon, K. S. Kim, J. S. Shin, J. S. Suh and J. Cheon, *J. Am. Chem. Soc*., 2005, **127**, 12387-12391.

176 S. Giri, B. G. Trewyn, M. P. Stellmarker and V. S. Y. Lin, *Angew. Chem. Int. Ed*., 2005, 44, 5038-5044.

177 J. Kim, J. E. Lee, J. Lee, Y. Jang, S. W. Kim, K. An, J. H. Yu and T. Hyeon, *Angew. Chem. Int. Ed*., 2006, **118**, 4907–4911.

178 T. Sen, A. Sebastianelli and I. J. Bruce, *J. Am. Chem. Soc*., 2006, **128**, 7130-7131.

179 M. Arruebo, M. Galan, N. Navascues, C. Tellez, C. Marquina, M. R. Ibarra and J. Santamaria, *Chem. Mater*., 2006, **18**, 1911-1919.

180 C. Y. Lai, B. G. Trewyn, D. M. Jeftinija, K. Jeftinija, S. Xu, S. Jeftinija and V. S. Y. Lin, *J. Am. Chem. Soc*., 2003, **125**, 4451-4459.

181 A. H. Lu, W. C. Li, A. Kiefer,W. Schmidt, E. Bill, G. Fink and F. Schuth, *J. Am. Chem. Soc.*, 2004, **126**, 8616-8617.

182 L. Zhang, S. Z. Qiao, Y. Jin, Z. Chen, H. Gu and Max Lu, *Adv. Mater*., 2008, **20**, 805–809.

183 S. Biju, Y. Eom, J. C. G. Bunzli and H. K. Kim, J. Mater. Chem. C, 2013, 1, 3454–3466.

184 W. Stoeber, A. Fink and E. Bohn, *J. Colloid Interface Sci*., 1968, **26**, 62-69.

185 M. Ide, E. D. Canck, I. V. Driessche, F. Lynenc and P. V. D. Voorta, *RSC Adv*., 2015, **5**, 5546–5552.

186 T. Salesch, S. Bachmann, S. Brugger, R. Rabelo-Schaefer, K. Albert, S. Steinbrecher, E. Plies, A. Mehdi, C. Rey, R. J. P. Corriu and E. Lindner, *Adv. Funct. Mater*., 2002, **12**, 132-142.

187 V. Rebbin, R. Schmidt and M. Froba, *Angew. Chem. Int. Ed*., 2006, **45**, 5210 –5214.

188 L. Huang, J. Lu, B. Di, F. Feng, M. Su and F. Yan, *J. Sep. Sci.*, 2011, **34**, 2523–2527

189 G. R. Zhu, Q. H. Yang, D. M. Jiang, J. Yang, L. Zhang, Y. Li and C. Li, *J. Chromatogr. A*, 2006, **1103**, 257–264.

190 Y. P. Zhang, Y. Jin, P. Dai, H. Yu, D. H. Yu, Y. X. Ke and X. M. Liang, *Anal. Methods*, 2009, **1**, 123–127.

191 Y. P. Zhang, Y. Jin, P. Dai, H. Yu, D. H. Yu, Y. X. Ke and X. M. Liang, *Talanta*, 2010, **81**, 824–830.

192 G. R. Zhu, D. M. Jiang, Q. H. Yang, J. Yang and C. Li, *J. Chromatogr. A*, 2007, **1149**, 219–227.

193 G. R. Zhu, H. Zhong, Q. Yang and C. Li, *Micropor. Mesopor. Mater.*, 2008, **116**, 36–43.

194 C. Li, B. Di, W. Q. Hao, F. Yan and M. X. Su, J. *Chromatogr. A*, 2011, **1218**, 408–415.

195 J. Lu, L. L. Huang, B. Di, F. Feng and M. X. Su, *Chromatographia*, 2011, **74**, 515–521.

196 A. Walcarius and L. Mercier, *J. Mater. Chem*., 2010, **20**, 4478–4511.

197 H. Zhu, D. J. Jones, J. Zajac, R. Dutartre, M. Rhomari and J. Roziere, *Chem. Mater*., 2002, **14**, 4886-4894.

198 M. Waki, N. Mizoshita, T. Ohsuna, T. Taniab and S. Inagaki, *Chem. Commun*., 2010, **46**, 8163–8165.

199 O. Olkhovyk and M. Jaroniec, *J. Am. Chem. Soc*., 2005, **127**, 60-61

200 M. C. Burleigh, Sheng Dai, E. W. Hagaman and J. S. Lin, *Chem. Mater*., 2001, **13**, 2537-2546.

201 P. J. Chiu, S. Vetrivel, A. S. T. Chiang and H. M. Kao, *New J. Chem*., 2011, **35**, 489–494.

202 S. A. Trammell, B. J. Melde, D. Zabetakis, J. R. Deschamps, M. A. Dinderman, B. J. Johnson and A. W. Kusterbeck, *Sensors and Actuators B*, 2011, **155,** 737–744.

203 S. A. Trammell, M. Zeinali, B. J. Melde, P. T. Charles, F. L. Velez, M. A. Dinderman, A. Kusterbeck and M. A. Markowitz, *Anal. Chem*., 2008, **80,** 4627–4633.

204 M. C. Burleigh, M. A. Markowitz, M. S. Spector and B. P. Gaber, *Environ. Sci. Technol*., 2002, **36**, 2515–2518.

205 S. Jayasundera, M. C. Burleigh, M. Zeinali, M. S. Spector, J. B. Miller, W. F. Yan, S. Dai and M. A. Markowitz, *J. Phys. Chem. B*, 2005, **109,** 9198–9201.

206 J. Peng, Y. Yao, X. Zhang, C. Li and Q. Yang, *Chem. Commun*., 2014, **50**, 10830-10833.

207 J. Du, J. C. Wechsler, J. M. Lobez, H. P. Loock and C. M. Crudden, *Small*, 2010, **6**, 1168–1172.

208 B. J. Melde and B. J. Johnson, *Anal. Bioanal. Chem*., 2010. **398**, 1565–1573.

209 S. S. Park, B. An and C. S. Ha, *Micropor. Mesopor. Mater*., 2008, **111**, 367–378.

210 B. J. White, M. Zeinali, K. M. Shafer, C. H. Patterson Jr., P. T. Charles and M.A. Markowitz, *Biosensors and Bioelectronics*, 2007, **22**, 1154–1162.

211 J. Lin, Z. Wei and C. Mao, *Biosensors and Bioelectronics*, 2011, **29**, 40– 45.

212 X. Qiu, S. Han, Y. Hu and B. Sun, *Chem. Eur. J.* 2015, **21**, 4126 – 4132.

213 E. D. Canck, C. Vercaemst, F. Verpoort and P. V. D. Voort, *Stud. Surf. Sci. Catal*., 2010, **175**, 365–368.

214 B. J. Johnson, N. E. Anderson, P. T. Charles, A. P. Malanoski, B. J. Malde, M. Nasir and J. R. Deschamps, *Sensors*, 2011 **11**, 886–904.

215 B. J. Johnson, B. J. Malde, G. W. Peterson, B. J. Schindl and P. Jones, *Chem. Eng. Sci*., 2012, **68**, 376–382.

216 M. Kubo, K. Ishiyama, A. Shimojima and T. Okubo, *Micropor. Mesopor. Mater*., 2012, **147**, 194–199.

217 C. B. Vidal, A. L. Barros, C. P. Moura, A. C. A. DeLima, F. S. Dias, L. C. G. Vasconcellos, P. B. A. Fechine and R. F. J. Nascimento, *Colloid. Inter. Sci*., 2011, **357**, 466–473.

218 Y. Tang and K. Landskron, *J. Phys. Chem. C*, 2010, **114**, 2494–2498.

219 K. Sim, N. Lee, J. Kim, E. B. Cho, C. Gunathilake and M. Jaroniec, *ACS Appl. Mater. Interfaces*, 2015, **7**, 6792−6802.

220 B. Camarota, P. Ugliengo, E. Garrone, C. O. Arean, M. R. Delgado, S. Inagaki and B. Onida, *J. Phys. Chem. C*, 2008, **112**, 19560–19567.

221 G. N. Kalantzopoulos, A. Enotiadis, E. Maccallini, M. Antoniou, K. Dimos, A. Policicchio, E. Klontzas, E. Tylianakis, V. Binas, P.N. Trikalitis, R.G. Agostino, D. Gournis and G.E. Froudakis, *Intl. J. Hydrogen Energy*, 2014, **39**, 2104- 2114.

222 D. Gust, T. A. Moore and A. L. Moore, *Acc. Chem. Res*., 2001, **34**, 40 – 48.

223 M. S. Choi, T. Yamazaki, I. Yamazaki and T. Aida, *Angew. Chem. Int. Ed*., 2004, **43**, 150-158.

224 A. Ajayaghosh and V. K. Praveen, *Acc. Chem. Res*., 2007, **40**, 644 –656.

225 H. Imahori, *J. Phys. Chem. B*, 2004, **108**, 6130 – 6143.

226 M. H. V. Huynh, D. M. Dattelbaum and T. J. Meyer, *Coord. Chem. Rev*., 2005, **249**, 457– 483.

227 S. Inagaki, O. Ohtani, Y. Goto, K. Okamoto, M. Ikai, K. Yamanaka, T. Tani and T. Okada, *Angew. Chem. Int. Ed*., 2009, **48**, 4042 –4046.

228 H. Takeda, Y. Goto, Y. Maegawa, T. Ohsuna, T. Tani, K. Matsumoto, T. Shimad and S. Inagaki, *Chem. Commun*., 2009, 6032–6034.

229 N. Mizoshita, Y. Goto, T. Tani and S. Inagaki, *Adv. Mater*., 2009, **21**, 4798–4801.

230 N. Mizoshita, Y. Goto, Y. Maegawa, T. Tani and S. Inagaki, *Chem. Mater*., 2010, **22**, 2548–2554.

231 P. N. Minoofar, B. S. Dunn and J. I. Zink, *J. Am. Chem. Soc*., 2005, **127**, 2656–2665.

232 X. Zhang, M. A. Ballem, Z. J. Hu, P. Bergman and K. Uvdal, *Angew. Chem. Int. Ed*., 2011, **50**, 5729 –5733.

233 L. Grosch, Y. J. Lee, F. Hoffmann and M. Froba, *Chem. Eur. J*. 2015, **21**, 331 – 346.

234 H. Inoue, T. Shimada, Y. Kou, Y. Nabetani, D. Masui, S. Takagi and H. Tachibana, *ChemSusChem*, 2011, **4**, 173 – 179.

235 J. H. Alstrum-Acevedo, M. K. Brennaman and T. J. Meyer, *Inorg. Chem*., 2005, **44**, 6802 –6827.

236 V. Balzani, A. Credi and M. Venturi, *ChemSusChem*, 2008, **1**, 26–58.

237 T. Hirai and M. Ota, *Mater. Res. Bull.,* 2006, **41**, 19–28.

238 M. Morishita, Y. Shiraishi and T. Hirai, *J. Phys. Chem. B*, 2006, **110**, 17898-17905.

239 H. Takeda, M. Ohashi, Y. Goto, T. Ohsuna, T. Tani and S. Inagaki, *Chem. Eur. J*., 2014, **20**, 9130 – 9136.

240 H. Takeda, M. Ohashi, T. Tani, O. Ishitani and S. Inagaki, *Inorg. Chem*., 2010, **49**, 4554–4559.

241 M. Ohashi, M. Aoki, K. Yamanaka, K. Nakajima, T. Ohsuna, T. Tani and S. Inagaki, *Chem. Eur. J*., 2009, **15**, 13041 – 13046.

242 Y. Ueda, H. Takeda, T. Yui, K. Koike, Y. Goto, S. Inagaki and O. Ishitani, *ChemSusChem*, 2015, **8**, 439 – 442.

243 Y. Lim, Y. S. Park, Y. Kang, D. Y. Jang, J. H. Kim, J. J. Kim, A. Sellinger and D. Y. Yoon, *J. Am. Chem. Soc*., 2011, **133**, 1375–1382.

244 H. Xia, M. Li, D. Lu, C. Zhang, W. Xie, X. D. Liu, B. Yang and Y. Ma, *Adv. Funct. Mater*., 2007, **17**, 1757-1764.

245 M. M. Shi, J. J. Lin, Y. W. Shi, M. Ouyang, M. Wang and H. Z. Chen, *Mater. Chem. Phys*., 2009, **115**, 841-845.

246 J. W. Kang, D. S. Lee, H. D. Park, Y. S. Park, J. W. Kim, W. I. Jeong, K. M. Yoo, K. Go, S. H. Kim and J. J. Kim, *J. Mater. Chem*., 2007, **17**, 3714-3719.

247 T. Yamanari, T. Taima, J. Sakai, J. Tsukamoto and Y. Yoshida, *Jpn. J. Appl. Phys*., 2010, **49**, 01AC02.

248 N. Mizoshita, M. Ikai, T. Tani and S. Inagaki, *J. Am. Chem. Soc*., 2009, **131**, 14225–14227.

249 S. Hamoudi, S. Royer and S. Kaliaguine, *Micropor. Mesopor. Mater*., 2004, **71**, 17-25.

250 Y. Guo, A. Mylonakis, Z. Zhang, G. Yang, P. I. Lelkes, S. Che, Q. Lu and Y. Wei, *Chem. Eur. J.,* 2008, **14**, 2909 – 2917.

251 Y. Lu, Fan, N. Doke, D. A. Loy, R. A. Assink, D. A. LaVan and C. J. Brinker, *J. Am. Chem. Soc*., 2000, **122**, 5258-5261.

252 B. D. Hatton, K. Landskron, W. Whitnall, D. D. Perovic and G. A. Ozin, *Adv. Funct. Mater*., 2005, **15**, 823-829.

253 W. Wang, D. Grozea, A. Kim, D. D. Perovic and G. A. Ozin, *Adv. Mater*., 2010, **22**, 99-102.

254 W. Wang, D. Grozea, S. Kohli, D. D. Perovic and G. A. Ozin, *ACS Nano*, 2011, **5**, 1267-1275.

255 M. Seino, W. Wang, J. E. Lofgreen, D. P. Puzzo, T. Manab and G. A. Ozin, *J. Am. Chem. Soc*., 2011, **133**, 18082–18085.

256 K. Landskron, B. D. Hatton, D. D. Perovic and G. A. Ozin, *Science*, 2003, **302**, 266-269.

257 F. Goethals, M. R. Baklanov, I. Ciofi, C. Detavernier, P. V. D. Voort and I. V. Driessch, *Chem. Commun.*, 2012, **48**, 2797–2799.

258 F. Goethals, I. Ciofi, O. Madia, K. Vanstreels, M. R. Baklanov, C. Detavernier, P. V. D. Voort and I. V. Driessche, *J. Mater. Chem.*, 2012, **22**, 8281–8286.